2010

Galaxy Zoo: Passive Red Spirals

Karen Masters
Haverford College, klmasters@haverford.edu

Moein Mosleh

A. Kathy Romer

Robert C. Nichol

Monthly Notices
of the
ROYAL ASTRONOMICAL SOCIETY

Mon. Not. R. Astron. Soc. **405,** 783–799 (2010) doi:10.1111/j.1365-2966.2010.16503.x

Galaxy Zoo: passive red spirals★

Karen L. Masters,[1]† Moein Mosleh,[2,3] A. Kathy Romer,[2] Robert C. Nichol,[1] Steven P. Bamford,[4] Kevin Schawinski,[5] Chris J. Lintott,[6] Dan Andreescu,[7] Heather C. Campbell,[2,1] Ben Crowcroft,[8] Isabelle Doyle,[1] Edward M. Edmondson,[1] Phil Murray,[9] M. Jordan Raddick,[10] Anže Slosar,[11] Alexander S. Szalay[10] and Jan Vandenberg[10]

[1]*Institute for Cosmology and Gravitation, Dennis Sciama Building, University of Portsmouth, Burnaby Road, Portsmouth PO1 3FX*
[2]*Astronomy Centre, University of Sussex, Falmer, Brighton BN1 9QJ*
[3]*Leiden Observatory, Leiden University, PO Box 9513, 2300 RA Leiden, the Netherlands*
[4]*Centre for Astronomy & Particle Theory, University of Nottingham, University Park, Nottingham NG7 2RD*
[5]*Einstein Fellow/Yale Center for Astronomy and Astrophysics, Yale University, PO Box 208121, New Haven, CT 06520, USA*
[6]*Oxford Astrophysics, Department of Physics, University of Oxford, Denys Wilkinson Building, Keble Road, Oxford OX1 3RH*
[7]*LinkLab, 4506 Graystone Ave., Bronx, NY 10471, USA*
[8]*Portsmouth Grammar School, High Street, Portsmouth PO1 2LN*
[9]*Fingerprint Digital Media, 9 Victoria Close, Newtownards, Co. Down, BT23 7GY*
[10]*Department of Physics and Astronomy, The Johns Hopkins University, Homewood Campus, Baltimore, MD 21218, USA*
[11]*Berkeley Center for Cosmological Physics, Lawrence Berkeley National Lab. & Physics Department, University of California, Berkeley, CA 94720, USA*

Accepted 2010 February 10. Received 2010 February 8; in original form 2009 October 19

ABSTRACT

We study the spectroscopic properties and environments of red (or passive) spiral galaxies found by the Galaxy Zoo project. By carefully selecting face-on disc-dominated spirals, we construct a sample of truly passive discs (i.e. they are not dust reddened spirals, nor are they dominated by old stellar populations in a bulge). As such, our red spirals represent an interesting set of possible transition objects between normal blue spiral galaxies and red early types, making up ∼6 per cent of late-type spirals. We use optical images and spectra from Sloan Digital Sky Survey to investigate the physical processes which could have turned these objects red without disturbing their morphology. We find red spirals preferentially in intermediate density regimes. However, there are no obvious correlations between red spiral properties and environment suggesting that environment alone is not sufficient to determine whether a galaxy will become a red spiral. Red spirals are a very small fraction of all spirals at low masses ($M_\star < 10^{10}$ M$_\odot$), but are a significant fraction of the spiral population at large stellar masses showing that massive galaxies are red independent of morphology. We confirm that as expected, red spirals have older stellar populations and less recent star formation than the main spiral population. While the presence of spiral arms suggests that a major star formation could not have ceased a long ago (not more than a few Gyr), we show that these are also not recent post-starburst objects (having had no significant star formation in the last Gyr), so star formation must have ceased gradually. Intriguingly, red spirals are roughly four times as likely than the normal spiral population to host optically identified Seyfert/low-ionization nuclear emission region (LINER; at a given stellar mass and even accounting for low-luminosity lines hidden by star formation), with most of the difference coming from the objects with LINER-like emission. We also find a curiously large optical bar fraction in the red spirals (70 ± 5 verses 27 ± 5 per cent in blue spirals) suggesting that the cessation of star formation and bar instabilities in spirals are strongly correlated. We conclude by discussing the possible origins

★This publication has been made possible by the participation of more than 160 000 volunteers in the Galaxy Zoo project. Their contributions are individually acknowledged at http://www.galaxyzoo.org/Volunteers.aspx

†E-mail: karen.masters@port.ac.uk

of these red spirals. We suggest that they may represent the very oldest spiral galaxies which have already used up their reserves of gas – probably aided by strangulation or starvation, and perhaps also by the effect of bar instabilities moving material around in the disc. We provide an online table listing our full sample of red spirals along with the normal/blue spirals used for comparison.

Key words: surveys – galaxies: active – galaxies: evolution – galaxies: photometry – galaxies: spiral.

1 INTRODUCTION

The advent of large galaxy surveys like the Sloan Digital Sky Survey (SDSS) in which photometry (and therefore colours) is readily available for millions of objects has led to the common use of optical colours to define 'early' and 'late'-type galaxy samples (e.g. Cooray 2005; Bundy et al. 2006; Croton et al. 2007; Lee & Pen 2007; Salimbeni et al. 2008; Simon et al. 2009). This method is particularly favoured because obtaining morphologies for large numbers of galaxies has until recently been impossible. This simplification is justified because it has been shown many times that the majority of galaxies follow a strict colour–morphology relation. For example, Mignoli et al. (2009) argued that 85 per cent of galaxies to $z \sim 1$ are either red, bulge-dominated galaxies or blue, disc-dominated galaxies; while Conselice (2006) showed a similar result for 22 000 low-redshift galaxies (both using automated methods for morphological classification).

However, the clear correlation between colour and morphology is surprising, given that the colours of galaxies are determined primarily by their stellar content (and therefore their recent star formation history, mostly within the last Gyr), while the morphology is primarily driven by the dynamical history. The clear link between colour and morphology then gives a strong indication that the time-scales and processes which drive morphological transformation and the cessation of star formation are strongly related – at least in most cases. In this paper, however, we consider a class of object (the red spirals) where the link described above appears to be broken.

Since the morphology–density relation was first quantified (Dressler 1980), many mechanisms have been proposed for the transformation of blue, star-forming, disc galaxies in low-density regions of the Universe, to red, passive, early type galaxies in clusters. A recent review of many of the proposed mechanisms, and the evidence supporting them, can be found in Boselli & Gavazzi (2006). Clearly two things must happen for a star-forming blue spiral galaxy to turn into a passive red early type. First, star formation must cease (which can indirectly alter the morphology by causing spiral arms and the disc in general to fade, possibly producing an S0 or lenticular from a spiral). Secondly, in order to produce a *bona fide* elliptical, the same or a different process must also dynamically alter the stellar kinematics of the galaxy.

The presence of an unusually red or passive (i.e. non-star forming) population of spiral galaxies in clusters of galaxies was first noted by van den Bergh (1976) in the Virgo cluster. Later studies of distant cluster galaxies in *Hubble Space Telescope* (*HST*) imaging also revealed a significant number of so-called 'passive' spiral galaxies with a lack of on-going star formation (Couch et al. 1998; Dressler et al. 1999; Poggianti et al. 1999). Passive late-type galaxies were identified at lower redshifts in the outskirts of SDSS clusters by Goto et al. (2003), using concentration as a proxy for morphology. Passive spirals in a cluster at $z \sim 0.4$ were studied by Moran et al. (2006) who found star formation histories from the *Galaxy Evolution Explorer* (*GALEX*) observations consistent with the shutting down of star formation from strangulation (as described by Bekki, Couch & Shioya 2002). Passive spirals have also been revealed in a cluster at $z \sim 0.1$ in the Space Telescope A9012/Galaxy Evolution Survey (STAGES), using *HST* morphologies Wolf et al. (2009), rest-frame near-ultraviolet–optical spectral energy distributions (SEDs; Wolf, Gray & Meisenheimer 2005) and 24 μm data from *Spitzer* (Gallazzi et al. 2009). In that series of papers, 'dusty red late types' and 'optically passive late types' are found to be largely the same thing, with a non-zero (but significantly lowered) star formation rate revealed by the infrared data.

Red spirals/late types have been studied in several recent papers (Lee et al. 2008; Cortese & Hughes 2009; Deng et al. 2009; Hughes & Cortese 2009) as well as Mahajan & Raychaudhury (2009) who talk about blue passive galaxies (i.e.galaxies with blue colours, but showing no indication of recent star formation in their spectra) which mostly appear to have late-type morphologies and have very recently shut down star formation. These might be the progenitors of the red spirals. Bundy et al. (2010) have studied the redshift evolution of red sequence galaxies with disc like components in the Cosmic Evolution Survey (COSMOS) and use it to estimate that as many as 60 per cent of spiral galaxies must pass through this phase on the way to the red sequence – making it an important evolutionary step.

The Galaxy Zoo project (Lintott et al. 2008) revealed the presence of a significant number of visually classified spiral galaxies which are redder than the blue cloud (between 16 and 28 per cent of the total galaxy population depending on environment; Bamford et al. 2009). In this paper, we study in more detail the physical properties and environments of this population of red spiral galaxies. Galaxies drawn from this population have the morphological appearance of spiral galaxies with a distinct spiral arm structure, but have rest-frame colours which are as red as a typical elliptical galaxy, indicating little or no recent star formation activity. We are studying these objects in order to identify the physical process which is most important in their formation.

It is clear that all spiral galaxies can be affected by various physical processes as they evolve – in this paper, we attempt to identify which are the most important for red spirals, asking how they are able to shut down star formation while retaining their spiral morphology. A list of possible mechanisms includes processes that depend on environment. (1) Galaxy–galaxy interactions: in high-density regions, there is an increased probability of interaction with other galaxies. Most major mergers destroy spiral structure (Toomre & Toomre 1972) unless they involve very gas-rich progenitors (Hopkins et al. 2009), but some interactions can be quite gentle (e.g. Walker, Mihos & Hernquist 1996), for example minor-mergers, tidal interactions etc. (2) Interaction with the cluster itself also occurs and can remove the gas which forms the reservoir for star formation. This can be due to tidal effects (e.g. Gnedin 2003) or interaction with the hot intercluster gas, either through thermal

evaporation (Cowie & Songaila 1977) or ram pressure stripping (Gunn & Gott 1972). (3) Processes like harassment (Moore et al. 1999) and starvation or strangulation (Larson, Tinsley & Caldwell 1980; Bekki et al. 2002) have also been shown to have a significant effect on late-type galaxies. Harassment refers to the heating of gas by many small interactions, while starvation or strangulation refers to the gradual exhaustion of disc gas after the hot halo has been stripped away. Both of these mechanisms occur at much larger cluster radii (i.e. lower densities) than the 'classic environmental effects. Internal mechanisms could be more important. For example, (4) the latest semi-analytical models of galaxy formation all invoke feedback from a central massive black hole [or active galactic nuclei (AGN)] to explain the most massive red elliptical galaxies (Granato et al. 2004; Silk 2005; Schawinski et al. 2006; Croton et al. 2006; Bower et al. 2006), although the effect of this process on disc galaxies has been studied less, it still may have some effect (Okamoto, Nemmen & Bower 2008). (5) Another culprit could be bar instabilities in spiral galaxies which drive gas inwards (e.g. Combes & Sanders 1981), and may trigger AGN activity and/or central star formation (e.g. Shlosman, Peletier & Knapen 2000), perhaps using up the reservoir of gas in the outer disc and making spirals red. (6) Finally, red spirals could simply be old spirals which have used up all their gas in normal star formation activities without having any major interactions. In normal spirals, the gas that feeds on-going star formation comes from infall of matter from a reservoir in the outer halo (Boselli & Gavazzi 2006). As first suggested by Larson, Tinsley & Caldwell (1980) and expanded by Bekki et al. (2002), the removal of gas from this outer halo ('strangulation' or 'starvation') will cause a gradual cessation of star formation proceeding over several Gyr.

We describe the sample and data along with the selection of the red spirals in more detail in Section 2. In Section 3, we discuss the stellar populations and star formation history of the red spirals. In Section 4, we discuss their environment and the environmental dependence of star formation. The impact of AGN is considered in Section 5, and bar instabilities are discussed in Section 6. In Section 7, we discuss the plausible mechanisms for formation of the red spirals and future directions which could be taken to distinguish between them. We present a summary and conclusions in Section 8. The adopted cosmological parameters throughout this paper are $\Omega_{\rm m} = 0.3$, $\Omega_\Lambda = 0.7$ and $H_0 = 70\,{\rm km\,s^{-1}\ Mpc^{-1}}$.

2 SAMPLE SELECTION AND DATA

The sample of visually classified spiral galaxies used in this paper is drawn from the Galaxy Zoo (GZ1) clean catalogue (Lintott et al. 2008) which, by an order of magnitude, is the largest morphologically classified sample of galaxies. To make this unprecedented sample, over 160 000 volunteers visually inspected images of SDSS galaxies independently via an internet tool [the original GZ1 sample was selected from the SDSS Data Release 6 (DR6); Adelman-McCarthy et al. 2008]. For more information on the classification process in GZ1 and the conversion of multiple classifications per galaxy to redshift bias corrected type 'likelihoods' see Lintott et al. (2008) and Bamford et al. (2009). In brief, we use the spiral likelihood $p_{\rm spiral}$ and (in order to tell if the spirals have visible spiral arms) the quantities $p_{\rm CW}$ and $p_{\rm ACW}$ which describe how likely the spiral is to have 'clockwise' or 'anticlockwise' arms, respectively.

We make a volume-limited sample of galaxies from the GZ1 catalogue by selecting only objects from the SDSS Main Galaxy Sample (Strauss et al. 2002) with spectroscopic redshift between $0.03 < z < 0.085$ and by limiting the sample to an absolute magnitude of $M_r < -20.17$. This redshift range is picked to remove problems with peculiar velocities at the low redshift end (which would bias distance dependent quantities) and the upper limit is chosen as a compromise between sample size and luminosity range (and also a redshift up to which reliable local densities – see below – are available).

Our photometric quantities are taken from the SDSS DR6 (Adelman-McCarthy et al. 2008). We use model magnitudes for colours, and Petrosian magnitudes for total luminosities. We also make use of shape/structural parameters from SDSS, namely the axial ratio (a/b) from the r-band isophotal measurement which is used as a proxy for disc inclination; and fracDeV (or $f_{\rm DeV}$) – the fraction of the best-fitting light profile which comes from the de Vaucouleurs fit (as opposed to the exponential fit) and which is used as a proxy for bulge size in these visually classified spirals (as discussed in Masters et al. 2010a).

SDSS 3-arcsec fibre spectra are available for all galaxies in our sample. We use equivalent widths (EW) and absorption line indices measured for SDSS DR7 spectra by the Max Planck Institute for Astrophysics (MPA)-Garching group whose methods are described in Tremonti et al. (2004).[1]

As an estimate of stellar mass, we use the empirical fit in Baldry et al. (2006) which gives a stellar mass-light ratio in the r band as a function of the $(u - r)$ colour of the galaxy (based on calculations of stellar masses from Kauffmann et al. (2003a) and Granato et al. (2004) using the Bruzual & Charlot (2003) stellar population models. Obviously, this is an oversimplification of the calculation of stellar masses, not taking into account the varied star formation histories of galaxies with the same colour and luminosity; however, the method does have the advantage of being simply related to only two measured physical properties of the galaxies (colour and luminosity).

The local galaxy densities used in this paper are identical to those used in Bamford et al. (2009). The details of the method are described in Baldry et al. (2006). Briefly, Σ_N is determined by $N/(\pi d_N^2)$, where d_N is the projected distance to the Nth nearest galaxy (with $M_r < -20$) within $cz \pm 1000\,{\rm km\,s^{-1}}$. The final value used, Σ, is the average of Σ_N for $N = 4$ and 5. These local densities include a correction for redshift incompleteness due to fibre collisions by considering the photometric redshift likelihood distributions for galaxies without spectra. Typical values of Σ range from 0.05 ${\rm Mpc^{-2}}$ in voids to 20 ${\rm Mpc^{-2}}$ in clusters (Baldry et al. 2006).

2.1 Selection of Red Spiral Galaxies

We wish to select from the GZ1 volume limited sample a subset of truly passive red disc-dominated spiral galaxies (i.e. not dust reddened, nor red because they are dominated by bulge emission). We use a cut in the spiral likelihood (corrected for the small bias described in the appendix of Bamford et al. 2009) of $p_{\rm spiral} \geq 0.8$. Two things can complicate the picture in a sample selected purely by colour and spiral likelihood.

(i) Dust reddening of edge-on spiral galaxies.
(ii) Contamination by early-type spirals and/or S0s.

Masters et al. (2010a) show that the impact of dust reddening can be significant for inclined spiral galaxies, and that spiral galaxies

[1] http://www.mpa-garching.mpg.de/SDSS/

with large bulges (as measured by fracDeV) are intrinsically red. Therefore with no cuts on inclination or bulge size, a red spiral sample will be dominated by inclined dust reddened spirals, and spirals with large bulges. We choose in this paper to study only the most face-on spiral galaxies, requiring $\log(a/b) < 0.2$. This will minimize the impact of dust reddening on the sample (although we note that even at face-on spirals can be dust reddened; for example Masters et al. 2010a find a median Balmer decrement of 0.3 ± 0.3 mag in the centres of face-on GZ1 spirals).

Both Lintott et al. (2008) and Bamford et al. (2009) show that contamination of S0s into the GZ1 clean spiral sample should be small – an estimate of 3 per cent contamination is made. Furthermore, we use fracDeV ≤ 0.5 to select 'discy spirals'. As illustrated in Masters et al. (2010a), using a small sample of GZ1 spirals with B/T from the Millennium Galaxy Catalogue (Liske et al. 2003) this selects spiral galaxies with $B/T < 0.25$ or of types ∼Sb–Sc (where this relation between typical B/T and Hubble type comes from Simien & de Vaucouleurs 1986). One caveat to note here is that both fracDeV and B/T are light-weighted quantities, so in using the same fracDeV limit for both red and blue spirals will results in the red spirals having a slightly *lower* upper limit in bulge *mass* fraction than the blue spirals. This slight bias should only make the conclusions below stronger, as the red spirals may on average be more disc dominated than the comparison blue spiral sample.

Finally, we require that spiral arms be visible to GZ1 users, using $p_{\rm CW} > 0.8$ or $p_{\rm ACW} > 0.8$. The presence of spiral arms gives an indication that these red spirals may have only recently stopped forming stars, since spiral structures are expected to persist for only a short time after star formation ceases [for example Bekki et al. (2002) found that spirals arms persisted for only a few Gyr after the gas which provides the reservoir for on-going star formation was removed].

We show in Fig. 1, the colour–magnitude diagram of the 'face-on' volume-limited clean GZ1 sample. The locus of the galaxy population is illustrated by the grey-scale contours, and the positions of visually classified spirals in the red sequence are hi-lighted. The best fit to the red sequence of early types ($p_{\rm el} \geq 0.8$) is $(g - r) = 0.73 - 0.02(M_r + 20)$, and the scatter is $\sigma = 0.1$ mag. We therefore define the blue edge of the red sequence as

$$(g - r) = 0.63 - 0.02(M_r + 20), \quad (1)$$

which is indicated by the solid line in Fig. 1, and define a red spiral as one redder than this limit. Since the limit depends on magnitude, we point out that in our definition a blue spiral with a high luminosity could actually be slightly redder than a red spiral with a low luminosity.

The colour cut used here to select red spirals is different from than that used by either Bamford et al. (2009), who used a cut in $(u - r)$ versus stellar mass, or Skibba et al. (2009), who used

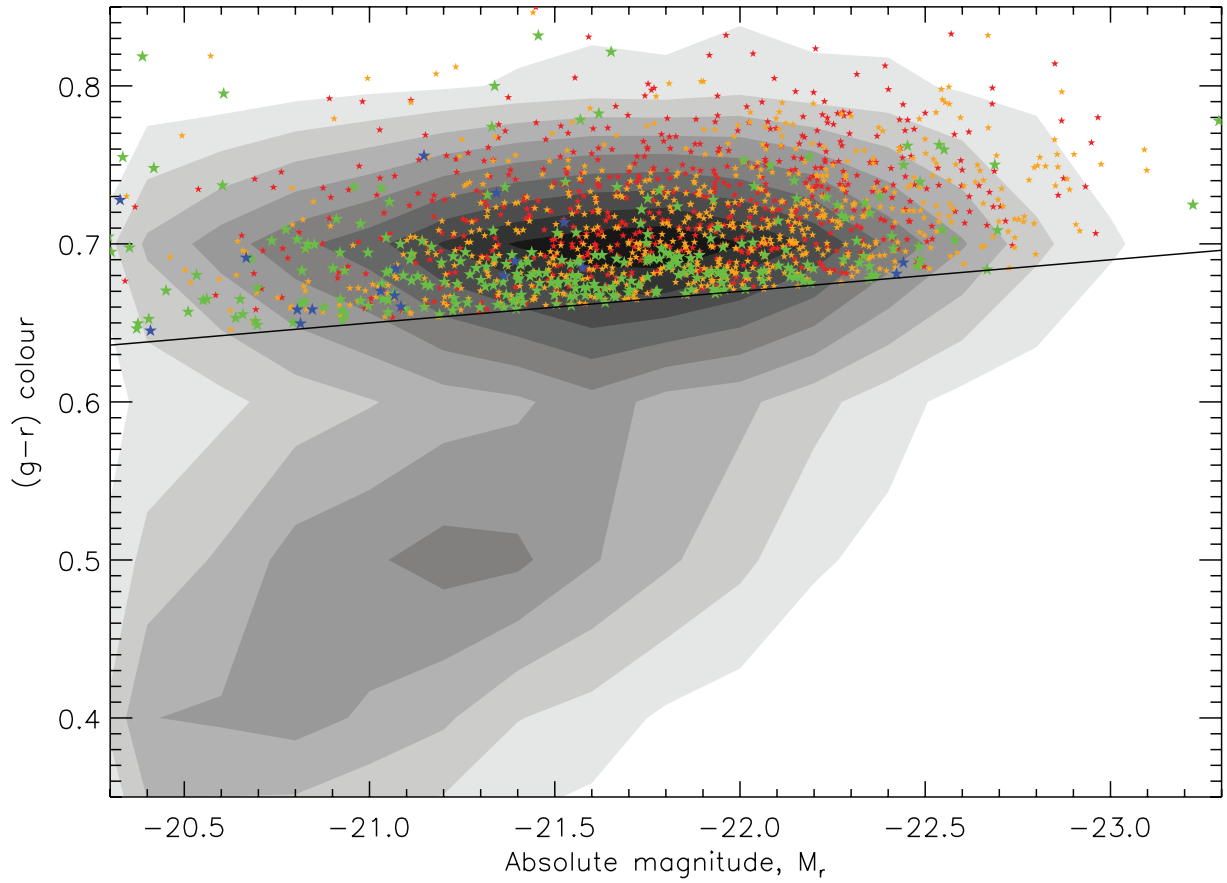

Figure 1. Colour–magnitude diagram of the 'face-on' [$\log(a/b) < 0.2$] volume limited clean GZ1 sample. The grey-scale contours show the location of galaxies in the red sequence and blue cloud. The solid line indicates the blue edge of the red sequence of GZ1 early types. All red spirals (having visible spiral arms) are shown colour coded by fracDeV (blue: $f_{\rm DeV} < 0.1$, which roughly corresponds to type Sd; green: $0.1 < f_{\rm DeV} < 0.5$, or Sb–Sc; orange: $0.5 < f_{\rm DeV} < 0.9$, or Sa–S0/a; red: $f_{\rm DeV} > 0.9$ which are spirals having very large bulges – but note that spiral arms are still visible here, so these are not S0s). Our final red spiral sample selects only those galaxies with $f_{\rm DeV} < 0.5$ (i.e.the blue and green points) to select against spirals dominated by light from the bulge.

k-corrected (to $z = 0.1$) magnitudes, which reddens the red sequence by $\sim$0.1 mag. Our cut is more conservative than either of those papers; they effectively select red spirals as being redder than most of the blue cloud, while we select red spirals to be as red as most elliptical galaxies. The difference in the two approaches is especially large at the low luminosity/stellar mass end of the galaxy population where (as can be seen in Fig. 1) the blue cloud is significantly bluer than the red sequence. However, the major difference in our sample and all previous ones used to study passive or red spirals is that we have made an effort to remove dust reddened inclined spirals, which has not been done before (e.g. Bamford et al. 2009; Skibba et al. 2009; Wolf et al. 2009).

Our final sample consists of 5433 face-on discy spirals with visible spiral arms, 294 of which (or 6 per cent) are classified as red. In what follows, we refer to the remaining 5139 spirals as our comparison sample a refer to them as either 'blue' spirals or 'normal' spirals. We provide an electronic table listing the SDSS names, positions and optical photometry parameters used in this paper for these two samples (our red spirals and comparison sample). A sample of this table is provided in the Appendix.

Fig. 2 shows the redshift, fracDeV (for bulge size), luminosity and stellar mass distributions of the red spirals compared to all spirals (in the face-on, discy sample). Red spirals are more likely to be found at the higher luminosity and larger fracDeV (and hence larger bulge) end of the spiral distribution showing that as is well known, luminous spirals with large bulges (earlier spiral types) are more likely to be red. There is a slight trend with redshift which can be explained by effect of the luminosity distribution in a volume-limited sample.

As also discovered by Wolf et al. (2009), red (or passive) spirals are an insignificant fraction of the total spiral population at stellar masses below $\sim 10^{10}$ $M_\odot$ (although note that Bamford et al. 2009 show that in the densest regions the few remaining low-mass spirals are mostly red), but are a significant fraction of spirals at large stellar masses. This shows that massive galaxies are red independent of morphology. However, we note here that this mass distribution may be slightly biased by our decision to classify spirals as red only if they are as red as ellipticals. This cut biases against low-mass red spirals as the blue cloud at low masses/luminosities moves further from the red sequence. Our sample is also incomplete for red objects below $10^{10.3}$ $M_\odot$ which corresponds to the luminosity limit for the reddest objects. Finally, we comment that the stellar population models of Bruzual & Charlot (2003) on which the Baldry et al. (2006) stellar masses are based, struggle to make red low-mass objects (since all their red objects must be very old, and therefore have very high mass-to-light ratios) so the use of this stellar mass estimate may anyway bias high the masses of the redder spirals. A more detailed modelling of the star formation history using stellar populations which account for the known populations of young red stars [the thermally pulsing asymptotic giant branch (TP-AGB)

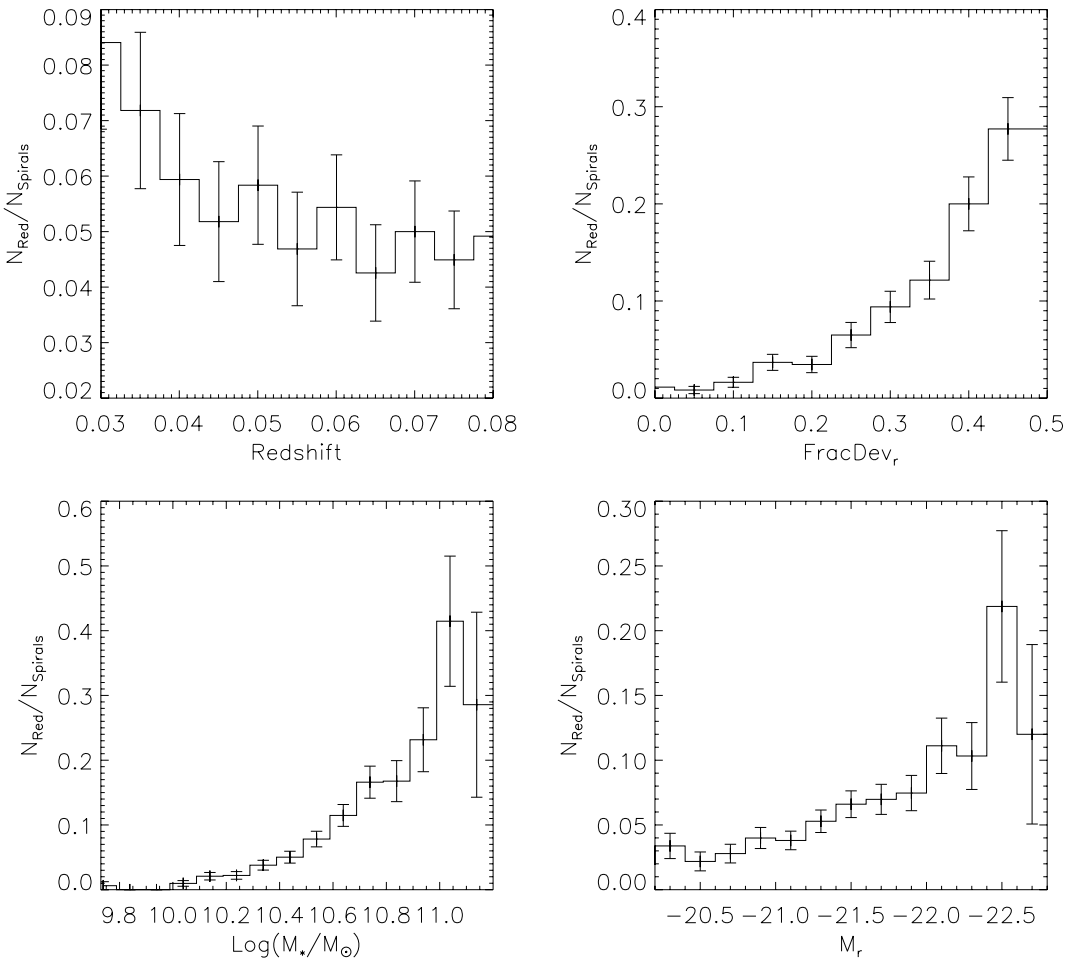

Figure 2. This figure shows the fraction of all face-on, discy GZ1 spirals which are found to be red (i.e. $N_{\rm red}/N_{\rm spiral}$) as a function of (1) redshift, (2) fracDeV (or bulge size), (3) stellar mass and (4) r-band absolute magnitude. $\sqrt{N}$ counting errors are shown.

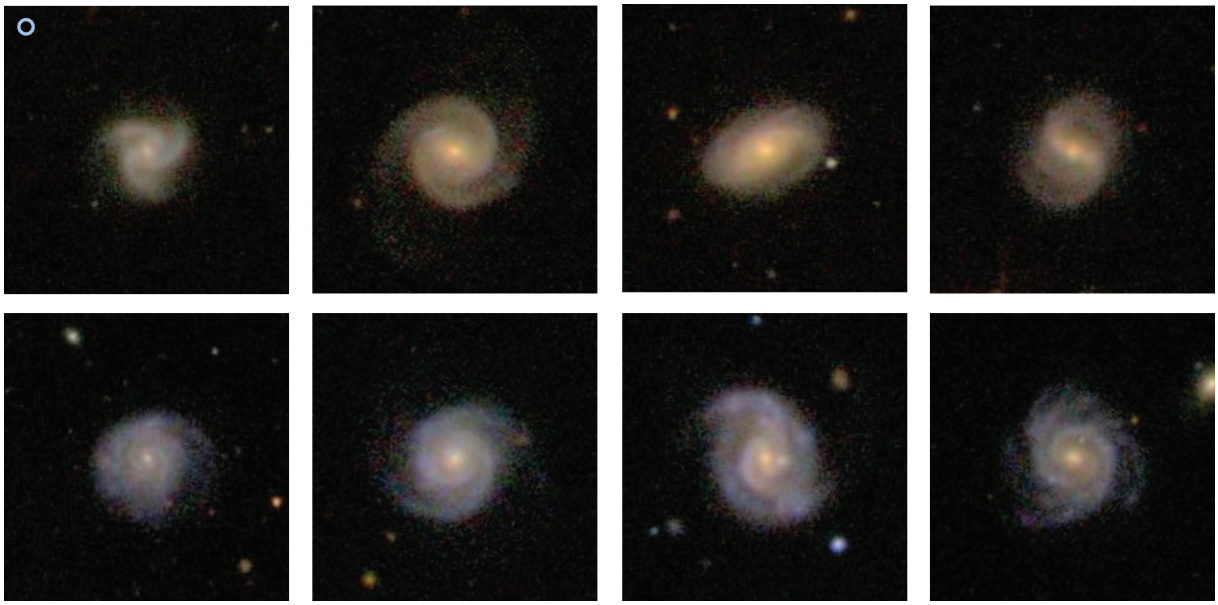

Figure 3. Top row: examples of face-on, red, discy spirals with visible arms (as described in the text), Bottom row: face-on, blue, discy spirals picked to have similar redshifts, absolute *r*-band magnitudes, angular sizes and fracDeV values as the red spiral immediately above them. Images are SDSS *gri* composites, all 1×1 arcmin^2 in size (these are some of the largest angular size galaxies in our sample). The size of the SDSS fibre is indicated at top left of the top-left image. Galaxies are (in red/blue pairs from left to right): SDSS J131428.83+334109.2 and SDSS J130058.63+395132.1 at $z \sim 0.04$, $M_r \sim -20.3$; SDSS J082959.05+304340.1 and SDSS J100515.00+513545.9 at $z \sim 0.05$ and $M_r \sim -21.7$; SDSS J104034.48+004902.6 and SDSS J123317.60+575620.1 at $z \sim 0.07$ and $M_r \sim -22.6$; and SDSS J134248.47+145553.5 and SDSS J155357.57+383923.9 at $z \sim 0.08$ and $M_r \sim -22.3$.

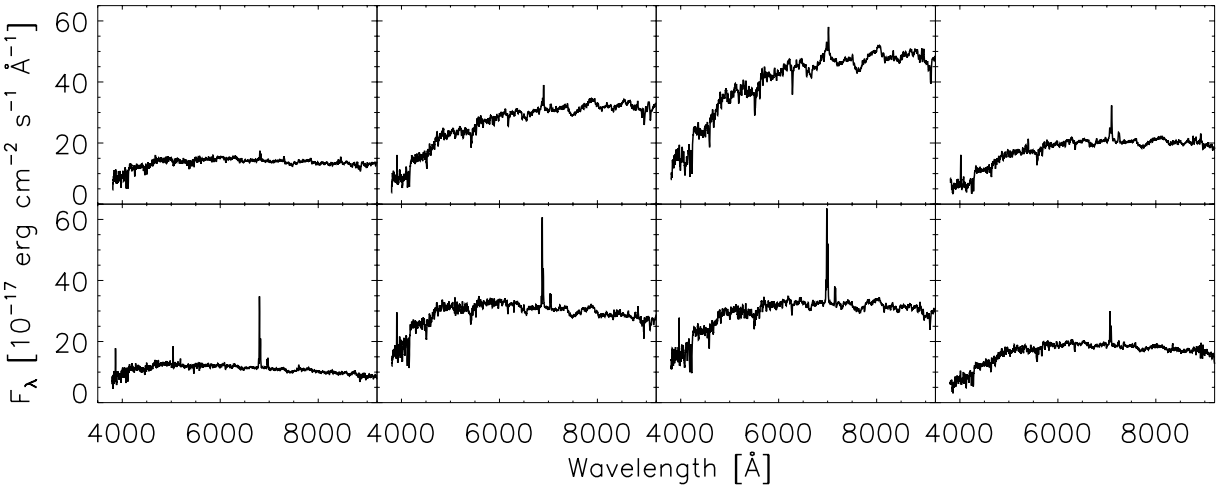

Figure 4. SDSS fibre spectra of the spirals shown in Fig. 3. Even in the central 3″, these spirals are clearly different in colour; the red spirals (top) mostly have continuum emission which increases towards long wavelengths (i.e. a red colour), while the blue spirals have continuum levels decreasing in that direction. Also note the significantly larger Hα emission in the spectra of the blue spirals (indicative of more on-going star formation), and the larger break at ∼4000 Å in the spectra of the red spirals (indicating an older stellar population).

phase included in Maraston (2005)] would provide more reliable stellar masses for these objects.

Fig. 3 shows example images of red and blue spirals from our sample of face-on discy spirals. The blue spirals shown have been picked to have similar redshifts and absolute magnitudes as the red spiral directly above them. A range of redshifts is shown. In these *gri* colour composite images, the colour difference between red and blue spirals is quite clear to the eye. Fig. 4 shows SDSS fibre spectra for the same galaxies in Fig. 3 (arranged in the same order), and even in this small sample it is clear that red spirals show less (but not zero) nebular emission from on-going star formation than the blue spirals (since they have smaller Hα emission lines) and have older stellar populations (the break at ∼4000 Å is larger in the red spirals than the blue spirals).

3 STAR FORMATION IN RED SPIRALS

In this section, we use the SDSS fibre spectra to study in more detail the star formation history and mean stellar age of 'red spiral' galaxies with reference to our comparison sample of blue spirals. Spectroscopic parameters are ideal for studying the stellar content of galaxies. A full star formation history model fit to the galaxy

spectra is beyond the scope of this paper, but absorption line indices such as $H\delta_A$ and the 4000 Å break strength provide information about stellar content and recent star formation history of a galaxy, while Hα and [O II] emission lines can indicate the presence of recent star formation.

3.1 Dust content

Before proceeding to use the spectral information to study the stellar content of the red spirals, we first want to check the dust content of the red spirals relative to the blue spirals. It is possible that the red colours of the spirals could be due to an enhanced amount of extinction and reddening from dust (even in our specially selected sample of face-on spirals designed to minimize dust effects) rather than an ageing stellar population from a lack of recent star formation. In fact Wolf et al. (2009) find that on-going star formation in their red spirals is obscured, although we note again that their objects include dust reddened inclined spirals which we have removed.

In order to quantify the levels of extinction, we compare the difference in flux between the first two lines in the Balmer series (Hα and Hβ). The expected flux ratio between these lines is $\Re_{\rm int} = F_\alpha/F_\beta = 2.76$, and has only a mild dependence on the temperature of the gas emitting the radiation (from $\Re_{\rm int} = 3.30$ at 2500° K to $\Re_{\rm int} = 2.76$ at 20 000° K; Osterbrock 1989). Therefore, deviations from the expected ratio can be used to measure the relative extinction between H_α (at 6562.8 Å in the *r* band) and H_β (at 4861.3 Å in *g* band). The relative extinction between these two wavelengths in magnitudes is

$$E(H_\beta - H_\alpha) = 2.5 \log \frac{\Re_{\rm obs}}{\Re_{\rm int}}, \quad (2)$$

which is equivalent to a colour in narrow band filters at these wavelengths.

In Fig. 5, we plot the Balmer decrements from the 3-arcsec SDSS fibre of blue and red spirals as a function of their stellar mass. This figure clearly indicates an increase in dust content of blue spirals as a function of stellar mass to a maximum at around $M \sim 10^{10.5}$ M$_\odot$. The trend is less clear in the red spirals where the numbers are significantly smaller, but tentatively supports a drop off in dust content for the highest mass objects (as also seen in Masters et al. 2010a). A negligible number of face-on spirals (either red or blue) have zero Balmer decrements in their central regions, showing that dust reddening always plays some role. However, we see no evidence for red spirals having significantly larger dust content than blue spirals at a given stellar mass (except perhaps in the lowest mass bin of the red spirals) and thus argue that the difference in colour is not due to differences in the dust content of the two populations.

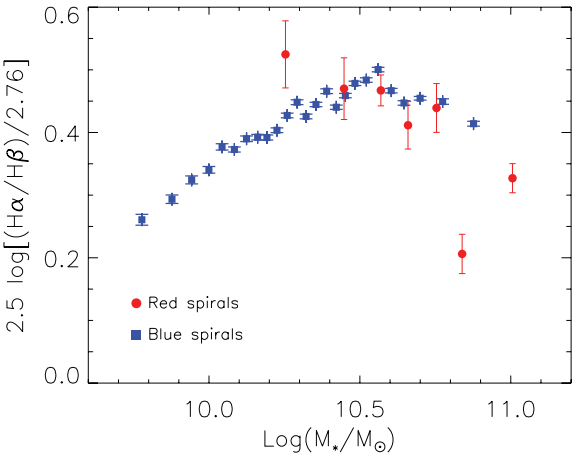

Figure 5. Balmer decrement in the SDSS fibre (expressed in magnitudes of extinction between Hα and Hβ) as a function of stellar mass for the blue (blue squares) and red (red dots) face-on discy spirals. Error bars indicate our estimate of the 1σ error on the median value.

3.2 Recent star formation history

Following the method in Kauffmann et al. (2003a), we use the Balmer absorption-line index $H\delta_A$ and the $D_n(4000)$ break to estimate mean stellar ages and recent star-burst activity of our sample.

The observed spectrum of a galaxy is the combination of flux from many stars. In galaxies with old stellar populations, there are a large number of stellar absorption lines (mostly from ionized metals) which crowd together at around 4000 Å. The 4000-Å break which they produce is the strongest discontinuity seen in the optical spectrum of a galaxy. In galaxies with a younger stellar population, there are many more hot stars, and the metals in them are multiply ionized. This significantly reduces the strength of the break, making it a good indicator of the mean age of a galaxy's stellar population. We follow Kauffmann et al. (2003a) and represent the strength of the 4000-Å break by the $D_n(4000)$ index (Balogh et al. 1999).

$H\delta_A$ absorption lines can be used to trace the recent ($\leq$1 Gyr) star formation activity of galaxies (Kauffmann et al. 2003a). $H\delta_A$ in the integrated galaxy spectra is almost entirely the contribution of A-type stars. The peak of this absorption feature thus occurs roughly 1 Gyr after a burst of star formation, once O and B stars have expired and the integrated light is dominated by A stars.

Histograms of the distribution of the two measurements for all the red and blue spirals are shown in Fig. 6. In Fig. 7, we plot $H\delta_A$ versus $D_n(4000)$ for our blue and red spirals samples split into four bins of stellar mass [starting at $\log(M_\star/M_\odot) = 10.3$ where the sample is completed for both red and blue spirals]. These figures illustrate that the red spirals, on average (luminosity weighted), have both older stellar populations and are less likely to have had significant bursts of star formation in the last Gyr [they have larger mean $D_n(4000)$ and smaller $H\delta_A$]. The data are overplotted on the models of Kauffmann et al. (2003a) showing the regions covered by their starburst (filled triangle), post-starburst (open triangle) and quiescent galaxies (filled squares). We can clearly see that red spirals at all masses are unlikely to fall in the part of the $D_n(4000)$–$H\delta_A$ plane which is occupied by starbursting or post-starbursting galaxies (i.e. they are not above the

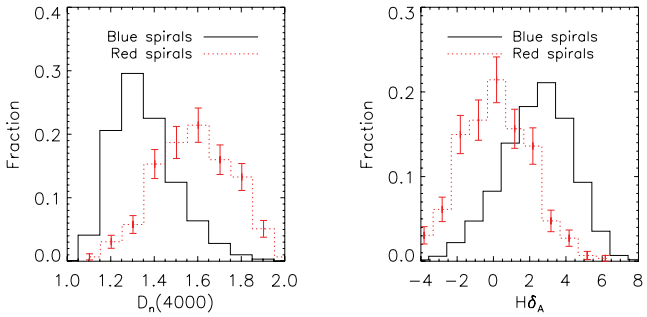

Figure 6. Histograms of the distribution of $H\delta_A$ and $D_n(4000)$ for the red and blue spiral samples (solid and dotted lines respectively). The y-axis shows the number in a given bin, relative to the total number in the respective sample. Counting errors are shown on the histogram for red spirals; due to the larger numbers of blue spirals the errors on those histograms are significantly smaller.

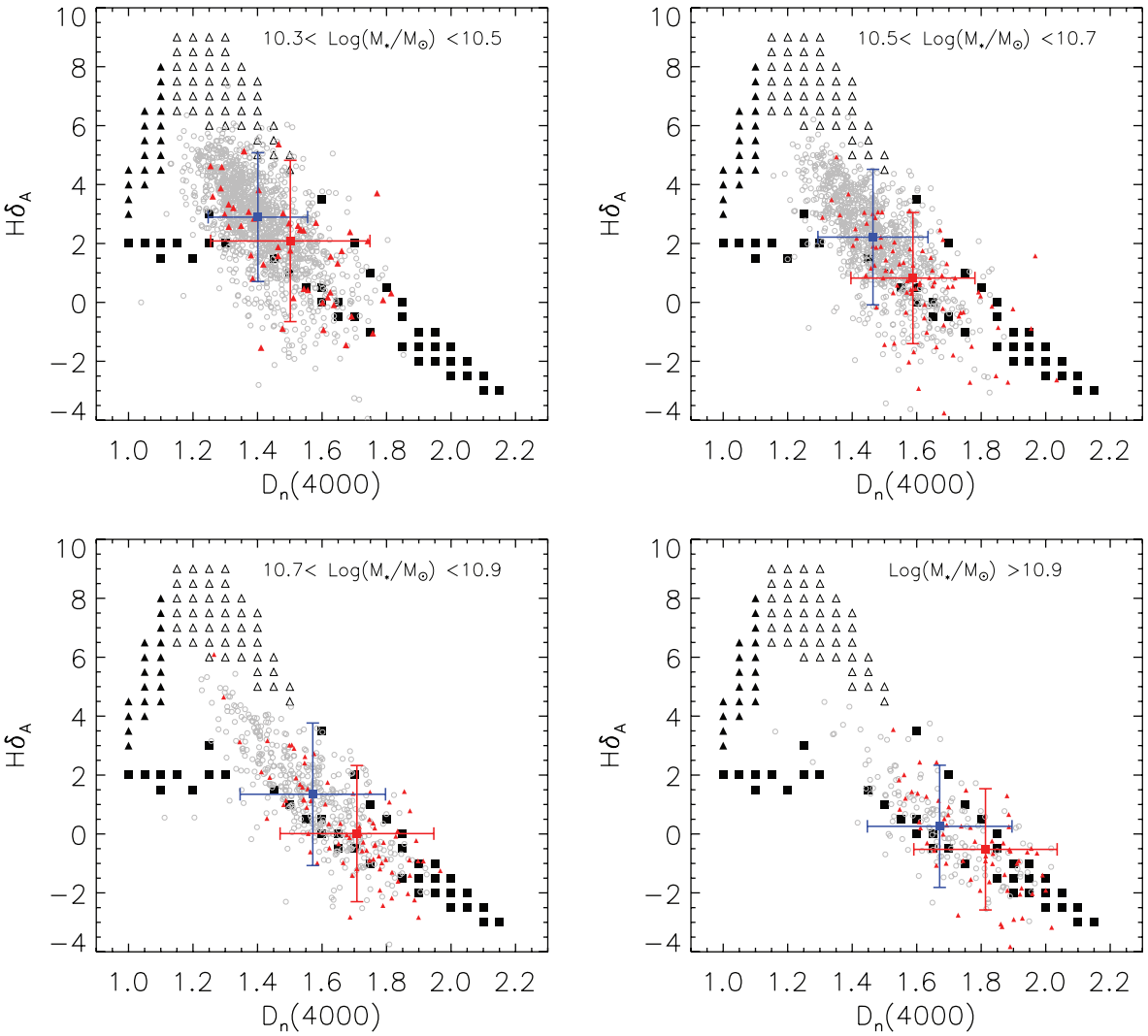

Figure 7. $H\delta_A$ versus $D_n(4000)$ is plotted for our sample of blue and red face-on, discy spirals. In each panel, the blue spirals are shown by grey circles, and the red spirals are shown by red triangles. The red and blue error bars indicate the interquartile ranges for the red and blue spirals, respectively. The different panels show the evolution with stellar mass, with the lowest mass galaxies at the upper left, down to the highest masses at the lower right. The red spiral galaxies on average show older stellar populations and less recent bursts of star formation in every mass bin. The data are plotted over galaxy models of Kauffmann et al. (2003a) showing regions covered by their starbursting (filled triangle), post-starburst (open triangle) and quiescent (filled squares) galaxies.

main locus of points), but that a significant fraction do lie in the part of the plane in which galaxies are expected to have formed an insignificant fraction of their stars in the last 2 Gyr (Kauffmann et al. 2003a), as well as in the mid-region where galaxies are expected to have mixed star formation histories (i.e. a mix of recent and much older star formation). In contrast, many of the blue spirals (especially at the lower stellar masses) are in the region of the plane occupied by galaxies with mixed star formation histories, although there are also starburst/post-starburst as well as more quiescent blue spirals.

Fig. 7 illustrates clearly the mass dependence of spiral star formation history; lower mass spirals are more likely to have had recent star formation. This is true for both red and blue spirals in our sample, however in any given mass bin the red spirals have both lower $H\delta_A$ and larger $D_n(4000)$ than equivalent blue spirals. It is clearly not stellar mass alone which is determining the star formation history of the red spirals.

The range of stellar ages of red spirals is similar to early-type galaxies [at least to the first order considering the range of $D_n(4000)$ – this does not account for metallicity effects which could cause a systematic offset] and they have not experienced recent burst of stars (in the last 1–2 Gyr); i.e. they are not post-starburst galaxies. However, the presence of spiral arms gives an indication that these red spirals must have recently been forming some stars, since spiral structures are expected to persist for only a short time after star formation completely ceases. The prevailing model for the origin of spiral structure in disc galaxies is the density wave theory proposed originally by Lin & Shu (1964). Discussing observations available at the time, which showed that galaxies without significant amount of interstellar gas do not have prominent spiral patterns, Lin & Shu (1964) suggest that any spiral structure, even if present in the old stellar population would not be visible, due to a lack of gas and star formation. More recent numerical simulations support this early picture of a relatively rapid fading of spiral arms after star formation ceases. For example, Bekki et al. (2002) found that spiral arms persisted for only a few Gyr after the gas which provides the reservoir for on-going star formation was removed. Observationally, Ishigaki, Goto & Matsuhara (2007) use spatially resolved

spectroscopy of the passive spiral SDSS J074452.52+373852.7 to show that this galaxy probably stopped forming stars about 1–2 Gyr ago – and it's spiral structure is still just visible. Follow-up integral field unit (IFU), and/or higher signal-to-noise ratio spectroscopy for a representative sample of the red spirals could measure population ages and test this picture further. Such work is planned.

In the red spirals, current star formation is significantly reduced compared to the normal/blue spirals, even at fixed stellar mass but it does not appear to have completely stopped in all objects (as we will see below). A major amount of star formation could not have ceased abruptly recently (as they are not post-starburst) or very long ago (more than a few Gyr because of the presence of spiral arms). It is therefore possible to conclude that star formation either ceased abruptly in the red spirals between the post-starburst and spiral arm fading time-scales (about one to a few Gyr ago) or that there has been a gradual cessation of star formation in the red spirals over the past few Gyr.

4 THE EFFECT OF ENVIRONMENT

The morphology–density relation (Dressler 1980) revealed that spiral galaxies favour lower density environments than early types. However, recent work (e.g. Ball, Loveday & Brunner 2008; Bamford et al. 2009; Deng et al. 2009; Skibba et al. 2009) has shown that the colour–density relation is stronger than the morphology–density relation (i.e. at a fixed morphology galaxies in higher density environments are redder, but at a fixed colour, there is little morphology–density dependence). We have already seen (Bamford et al. 2009; Skibba et al. 2009) that GZ1 red spirals are more common in high-density regions (and conversely blue early types are more common in low-density regions; Schawinski et al. 2009b). There are also clear suggestions in both Bamford et al. (2009) and Skibba et al. (2009) that the peak of the red spiral distribution occurs in intermediate density regions. Therefore, environment is clearly a candidate for driving the process which turns spirals red. As discussed in Section 1, various environmental mechanisms have been proposed to suppress star formation and turn galaxies red in high-density regions. In this section, we will consider the effect of environment on the red spirals in particular, looking at their preferred locations, and tracers of their star formation as a function of local density.

4.1 The environments of red spirals

In Fig. 8, we present the fraction of galaxies in our red and blue spiral samples (relative to the full volume limited galaxy sample) versus the local galaxy density. We confirm the previous findings that red spiral fraction increases with local galaxy density, along with the well-established observation that the fraction of blue (or normal) spirals decreases. This figure suggests that the red spiral fraction peaks at intermediate densities, around $\Sigma = 1$ Mpc^{-2}, inside the infall radius of a typical cluster, but not in their cores (see fig. 5 of Bamford et al. 2009 for the correlation of Σ with the distance to the nearest cluster centre, this level of Σ corresponds to $d \sim 5$–15 Mpc depending on the richness of the cluster – for example it could be quite close in to a poor group or much further away from a rich cluster). In order to look at the impact of close neighbours, and not just local density, we also consider the (projected) distance to the nearest neighbour (within 100 km s^{-1} in the SDSS DR6 Spectroscopic Galaxy Sample). Fig. 9 shows the fraction of red and blue spirals in our face-on discy spiral sample as a function of this distance, showing that red spirals are a lot more likely to have close neighbours than blue spirals. (Of course Σ and the distance to the nearest neighbour are correlated – galaxies with a higher Σ will naturally have a nearer closest neighbour, and we have not attempted to disentangle the two measurements here.)

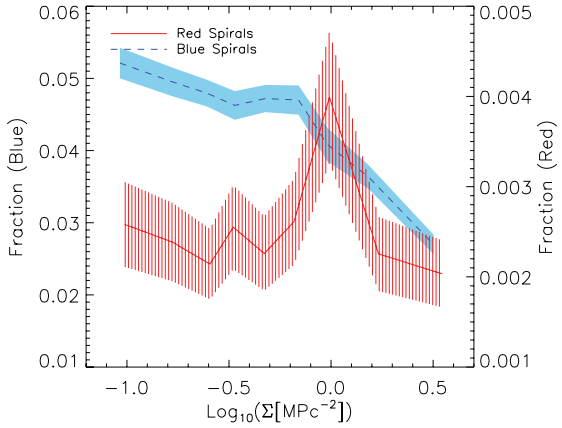

Figure 8. Fraction of red spiral galaxies (red solid line) and blue spirals (blue dashed line) relative to all types of SDSS galaxies in our volume limited sample plotted versus environment as measured by Σ. The error regions are also shown; note that the binning is the same for both red and blue spiral samples, and adjusted to have ∼30 red spirals per bin.

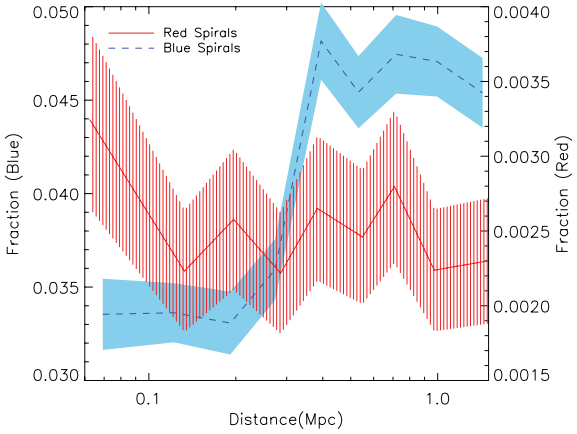

Figure 9. Fraction of red spiral galaxies (red solid line) and blue spirals (blue dashed line) relative to all types of SDSS galaxies in our volume limited sample as a function of projected distance to nearest neighbour. The error regions are also shown; note that the binning is the same for both red and blue spiral samples, and adjusted to have ∼30 red spirals per bin.

4.2 Environmental dependence of star formation

We now study the environmental dependence of star formation tracers in our samples of red and blue spirals. In Fig. 10, we show the median EW of [O II] and Hα as a function of local galaxy density for both blue and red face-on discy spirals.

At all densities, red spirals have significantly lower but *non-zero* EW in these two tracers of on-going star formation, but interestingly there are no significant trends with local density in either population, neither do we see any evidence for a change in the distribution of the quantities with environment (consistent with the findings of Bamford et al. 2008 for Hα in the galaxy population as a whole). There is perhaps a hint that the [O II] EW decreases with density for red spirals – a straight line fit to this trend has a $\sim 2\sigma$ significance

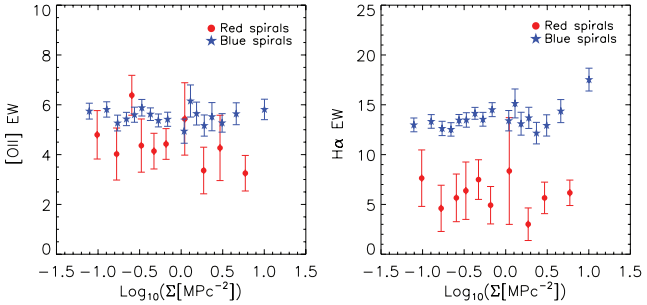

Figure 10. The median EW of [O II] and Hα as a function of local galaxy density. Blue and red spirals are shown as blue stars/red dots, respectively. Error bars show our estimate of the 1σ error on the median value.

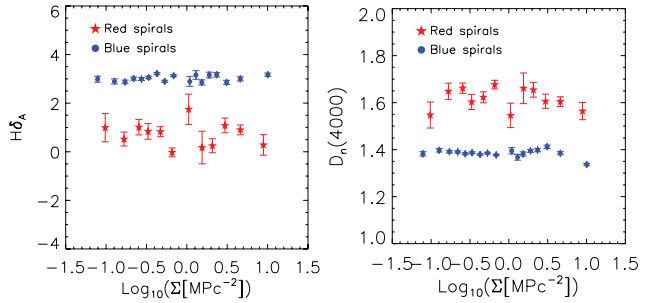

Figure 11. Median values of H$\delta_{\rm A}$ (a tracer of recent star formation) and $D_n(4000)$ (a tracer of average stellar age) as a function of local galaxy density. Blue and red spirals are shown as blue stars/red dots respectively. Error bars show our estimate of the 1σ error on the median value.

(a slope of -1.0 ± 0.4). We also see a slight increase in the Hα EW in blue spirals at very high density, which may be related to interaction triggered star formation in this population – or perhaps a higher rate of AGN contamination in blue spirals in high-density regions. This figure includes all galaxies, including those classified as AGN by their optical spectra (see Section 5), however in Section 5 we will show that there is a higher AGN fraction in the red spirals than the blue, so removing AGN contamination from these lines will only make the difference between red and blue spirals stronger.

Fig. 11 shows similar relations to that shown in Fig. 10 for the tracers H$\delta_{\rm A}$ and $D_n(4000)$ (as discussed in Section 3, these are tracers of recent starbursts and the mean age of the stellar population, respectively). Again we see that at all densities these indicators show less recent star formation and older stellar populations in red spirals than blue spirals, and that there are no significant trends with density in either population. We have repeated this exercise using (projected) distance to the nearest neighbour, and find similar results.

Red spirals in all environments have lower rates of recent and on-going star formation than blue spirals. This suggests that despite the increased fractions of red spirals in high-density regions, environment is not the only factor in the shutting down of star formation in red spirals – i.e. the main physical process cannot only happen in high-density regions (ruling out ram pressure stripping as the dominant process) and neither can it proceed faster in higher densities.

Our data are consistent with the process that turns spirals red being more likely to happen in high-density regions as long as it is possible and proceeds in the same fashion in all environments. Both gentle interactions, and/or strangulation mechanisms could explain these observations.

5 THE IMPACT OF AGN

The most recent semi-analytic models for galaxy formation all invoke some form of AGN feedback which inhibits star formation in the most massive, red (early-type) galaxies (Granato et al. 2004; Silk 2005; Croton et al. 2006; Bower et al. 2006) in order to match the number counts and properties of these objects in the local universe. Observational evidence now exists to support this hypothesis, showing that the AGN fraction peaks in the region between the blue cloud and the red sequence (Schawinski et al. 2007, 2009a). Could AGN feedback be responsible for the shutdown of star formation in the red spirals?

We test this by using emission line diagnostic diagrams (Baldwin, Phillips & Terlevich 1981, hereafter BPT; Veilleux & Osterbrock 1987; Cid Fernandes et al. 2001; Kewley et al. 2001, 2006) to probe the dominant source of ionization in the red and blue spiral galaxies. For this study, we restrict our analysis to galaxies with greater than 2σ emission line detection for all four lines used in the BPT diagram (i.e. [O III], Hα, [N II] and Hβ). Likewise, in order to reduce the effect of aperture bias of the SDSS 3-arcsec fibre on the BPT diagram, we shift the lower redshift range of our sample up from $z > 0.03$ to >0.05. This reduces the sample size to 181 (60 per cent) of the red spirals, and 3462 (66 per cent) of the blue spirals.

Standard emission line diagnostic diagrams (e.g. Kauffmann et al. 2003b; Schawinski et al. 2007) are used to divide galaxies whose budget of ionizing photons is dominated by current star formation (i.e. ionization from OB associations) and those whose interstellar medium is excited by other processes. These other processes include AGN, but also shocks and evolved stellar populations such as post-AGB stars, extreme horizontal branch stars, white dwarfs (Stasińska et al. 2008; Sarzi et al. 2010).

Observationally, the area between these two regions is populated by transition or composite objects where the total contribution to the ionizing budget from star formation and other processes is roughly comparable. Kewley et al. (2001) give a prescription based on theoretical modelling of starburst galaxies which indicates the region of the diagram which can be explained by starburst emission (to the lower left of the line), while Kauffmann et al. (2003b) made an empirical fit to the observed separation between the populations in SDSS galaxies, which is often used as a lower limit for the location of AGN. Here as a short hand, we will call objects to the upper right of the Kewley et al. (2001) line 'AGN' (even if other processes may be more important in some objects) or sometimes 'Seyfert+LINER' (as explained below), objects below the Kauffmann et al. (2003b) line 'star-forming' and objects falling between the two lines 'composite' objects.

The region dominated by ionization from processes other than star formation is furthermore divided into Seyferts and LINERs (low-ionization nuclear emission-line regions; Heckman 1980). To split this region into Seyfert and LINER types, we use the diagonal dividing line suggested by Schawinski et al. (2007). Objects in the Seyfert region are clearly identified as classical obscured (Type 2) Seyferts (i.e. AGN), while the LINER region is more controversial and possibly represents a heterogeneous population (see section 6 of Ho 2008 for a recent review of possible sources of ionization for LINERs). Recent results from the SAURON survey by Sarzi et al. (2010) show that the extended LINER emission seen in the most SDSS fibre spectra (whose physical footprint corresponds to 2–3 kpc in the sample studied here) is inconsistent with a central point source for the ionization, ruling out nuclear activity as the dominant source for the emission. Intriguingly, this is even the

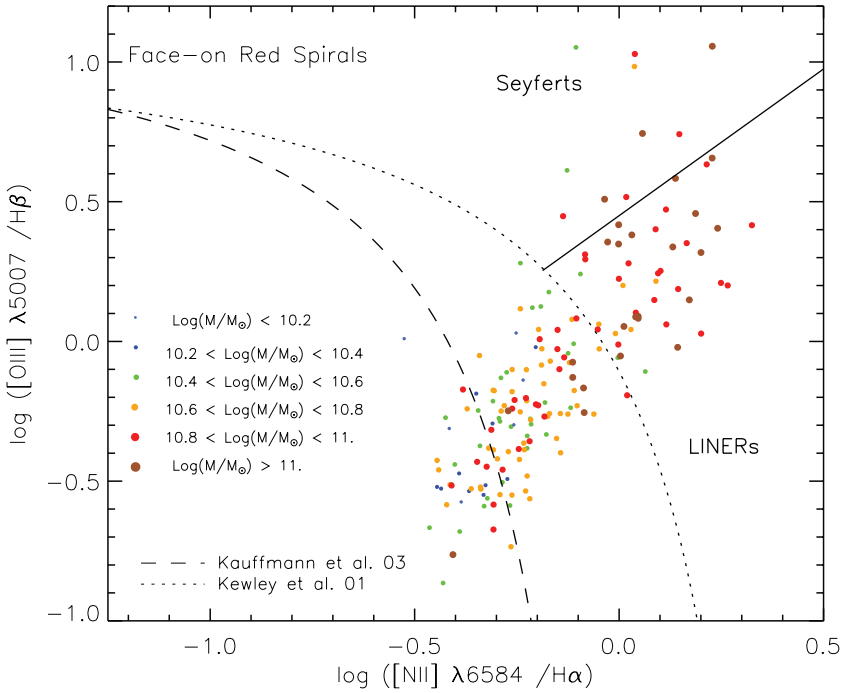

Figure 12. Distribution of face-on discy red spiral galaxies in the BPT diagram. The size and colour of the points indicate the stellar mass of the galaxies (as labelled). The diagonal dividing line for LINERs/Seyferts is taken from Schawinski et al. (2007).

case when the presence of nuclear activity (e.g. from radio data) is detected.

The position of red spirals on a BPT diagram is illustrated in Fig. 12 where points are coded (both in size and colour) by the stellar mass of the galaxy. Many more of the red spirals than the blue are placed above the Kewley et al. (2001) dividing line, indicating that they are not dominated by the emission from star-forming regions, but their gas must be ionized by other mechanisms (30 ± 4 per cent[2] of all face-on discy red spirals in redshift interval of 0.05–0.085, compared to 4 ± 1 per cent of blue spirals). As the plot indicates, a significant fraction of these galaxies are LINER type (82 ± 12 per cent). The remaining red spirals have many more composite objects than are found in the normal spiral population (49 ± 5 per cent compared to 15 ± 1 per cent of blue spirals) with only a relatively small fraction being classed as star-forming by the Kauffmann et al. (2003b) criterion (21 ± 3 per cent of red spirals compared to 81 ± 2 per cent of blue spirals).

Part of these trends can be explained by the larger stellar masses of the red spirals, since it is well known that Seyferts and LINERs are more common in higher mass galaxies (e.g. Kauffmann et al. 2003b). Therefore, for a fair comparison, we construct a sample of blue spirals selected from the full blue spiral population in such a way that they have the same mass distribution as the red spirals (our 'mass-matched' blue spiral sample). We show 181 of these galaxies (i.e. the same number as in the red spiral sample for ease of comparison) on the BPT diagram in Fig. 13. Compared to this mass-matched sample of blue spirals, red spirals are still significantly more likely to host optically identified Seyfert+LINER emission lines. Recall, 30 ± 4 per cent of red spirals are above the Kewley et al. (2001) division and 48 ± 5 per cent are in the composite region. In comparison, we find only 7 ± 1 per cent mass-matched blue spirals in the Seyfert+LINER region, and 23 ± 1 per cent in the composite region. Red spirals are therefore $\sim$4 times as likely to have Seyfert+LINER emission lines, and twice as likely to be composite objects when compared to similar blue spirals.

We plot in Fig. 14 the observed fractions of Seyfert+LINER and star-forming galaxies as a function of mass for both the red and blue spirals. For both subpopulations, the Seyfert+LINER fraction increases with stellar mass, while the star-forming fraction decreases, however as previously commented, at a given stellar mass red spirals are roughly twice as likely to be classified as Seyfert/LINER, and less likely (roughly half as likely) to be classified as a star-forming. There is a suggestion that the increase of Seyfert+LINER fraction with mass is also faster in the red spirals than it is in the blue spirals (at the expense of 'composite' objects, since the star-forming fractions are seen to decrease at approximately the same rate).

AGN fractions in all galaxies have generally been shown to be independent of environment (Miller et al. 2003; Sorrentino, Radovich & Rifatto 2006). However, recent work on X-ray selected AGN does suggest an environmental dependence such that X-ray selected AGN are more common in groups than clusters (Arnold et al. 2009, this work also comments on the complete disjoint of X-ray selected and BPT selected AGN samples making such studies hard to compare), and Lee et al. (2010) also suggest AGN are less common in higher densities. Here, we see no signature of a density dependence of the Seyfert+LINER fraction of red spirals, although we note that the red spiral sample is quite small to divide in this way and covers only a limited range of densities.

Red spirals with emission lines, which are not classified as coming from star formation, are more likely to be classified as LINERS than similar objects in the blue spirals population, with 82 ± 12 per cent of those in red spirals being LINERS versus 57 ± 7 per cent

[2] Errors on the fractions given in this section and elsewhere are $\sqrt{N}$ counting errors. This obviously breaks down when fractions approach zero or one, however for the purposes of this paper the approximation of the errors is adequate.

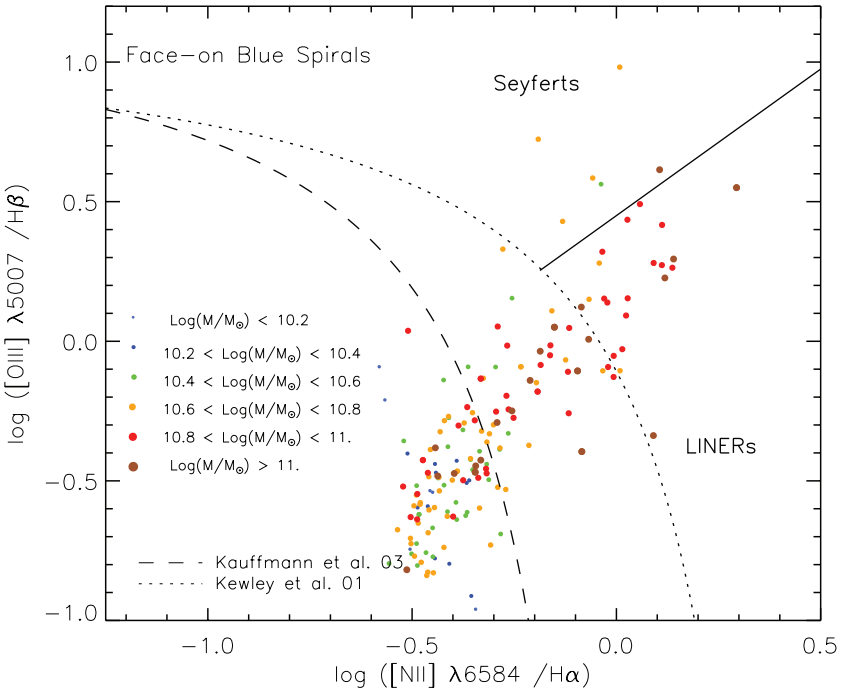

Figure 13. Distribution on the BPT diagram of our sample of face-on discy blue spiral galaxies with the same number of objects in each mass bin as the red spirals shown in Fig. 12 (selected randomly). The size and colour of the points indicate the stellar mass of the galaxies (as labelled).

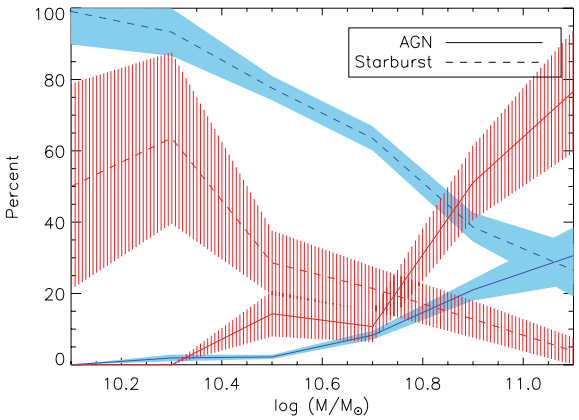

Figure 14. Fraction of galaxies in a given stellar mass range which are classified as 'AGN' (Seyfert+LINER) or star-forming from the BPT diagram (expressed as a percentage; note that the fraction classified as composites are not shown). The trends for blue spirals are shown with the blue lines, red spirals by the red lines. Shaded regions show the $\sqrt{N}$ counting errors on the fractions. Obviously, these errors break down where the fractions approach zero or one, but give a reasonable estimate elsewhere.

in the mass-matched blue spirals. This means the Seyfert fractions of red and blue spirals of the same mass are actually quite similar (6 ± 2 per cent of red spirals versus 3 ± 1 per cent of blue spirals) – the main difference in the two populations appears to be in the LINER fraction which suggests a link between LINER emission and the shutting down of star formation in spiral galaxies. Overall 25 ± 4 per cent of the red spirals are classified as having LINERs, while only 4 ± 1 per cent of the (mass matched) blue spirals meet the LINER criteria. Interestingly in visually classified early type galaxies, Schawinski et al. (2007) also found that an increase in LINER fraction was associated with 'stellar quiescence', while Smolčić (2009) studying radio loud AGN also found that the radio AGN in the red sequence were dominated by low-ionization AGN which were classified as LINERs in the BPT diagram.

The Balmer line emission from even a small amount of star formation is expected to dominate any AGN emission. Schawinski et al. (2010) study the masking of AGN (Seyfert) emission in star-forming galaxies and show that for AGN [O III] luminosities below 10^{39} erg s^{-1} most galaxies with star formation present will not be classified as AGN, and that only above 10^{40} erg s^{-1} will the sample of AGN identified by optical emission lines be reasonably complete in the blue cloud. We show in Fig. 15 histograms of the [O III] luminosities (extinction corrected using the method described in

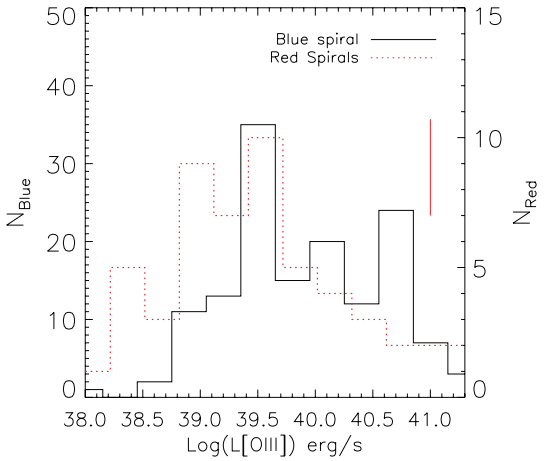

Figure 15. Histogram of [O III] luminosities of optically identified Seyferts and LINERS in the red spirals (red dotted line) and blue spirals from the mass matched sample (black solid line). The typical error on the red spiral histogram is indicated, offset for illustration purposes. Note that the *y*-axes are scaled such that the total area under each histogram is equal.

Lee et al. 2010) of both red and blue spirals (from the sample matched in mass with the red spirals) classified as having either Seyfert or LINER emission. This diagram suggests that there may be a difference in the luminosities of the emission lines identified in the two populations, such that fainter lines (below about $10^{39.3}$ erg s^{-1}) are found in the red spiral population which are not found in the blue spiral population. However, since the actual number of red spirals is small, the histograms do agree within the error.

If true, the above observation suggests that at least some LINERs are being revealed in the red spiral population either because the emission lines are no longer dominated by star formation or perhaps because the smaller amount of recent star formation means there is less dust shrouding the AGN. However, the difference cannot account for all of the extra LINERs in the red spirals – i.e. even at the luminous end of the distribution where we would not expect LINERs to be hidden in the blue spirals, we find more LINERs in red spirals (considering only emission with L[O III] $>10^{39}$ erg s^{-1} we find 24 ± 4 per cent of the red spirals have emission not consistent with star formation compared to 7 ± 1 per cent of the mass matched blue spirals), so we are able to say that at least high luminosity LINER emission is correlated with the shutting down of star formation in spiral galaxies.

Since we do not have either integral field observations or X-ray/radio data of red spirals, we present two alternative interpretations for the high LINER fraction in red spirals.

(i) *Photoionization from evolved stellar populations.* If we assume that the LINER emission in red spirals is mostly due to photoionization from evolved stellar populations (e.g. Stasińska et al. 2008), then we can naturally account for the relatively higher fraction of LINERs in red compared to blue spirals in the following way: in massive galaxies, there is a substantial component of hard ionizing radiation coming from evolved stellar populations, that would, in the absence of other factors, produce a weak LINER spectrum. In blue spiral galaxies, this signature is mostly overwhelmed by ongoing star formation, whereas in red spirals, where star formation has been gently quenched, no such competing source of photons is available.

(ii) *Low-luminosity nuclear activity.* If we assume that the LINER emission in red spirals is due to photoionization from a low-luminosity, low-Eddington AGN (e.g. Kewley et al. 2006), we can ask about the role of this AGN in the evolution of red spirals. As suggested earlier, red spirals gently quenched their star formation in an extended process that began about 2 Gyr in the past. This in turn implies that the *current* LINER AGN cannot be responsible for the suppression of star formation as it is happening now – with a substantial time delay after the quenching process. A similar, though shorter time delay is seen between the suppression of star formation and the start of substantial black hole growth (Schawinski et al. 2007). The LINER phase in red spirals, like in early-types (Schawinski et al. 2007), seems to be a post-quenching phenomenon. The interesting question then becomes why the particular internal environments of red spiral galaxies that have already quenched their star formation are so conducive to low-level black hole growth.

Further observations of red spirals are required to fully distinguish between these two interpretations. Spatially resolved spectroscopic observations (long-slit or IFU) are needed to test whether the LINER emission in red spirals is spatially extended as it is in early types. Deep X-ray or radio observations could yield evidence for on-going black hole accretion.

6 BAR FRACTIONS IN RED/BLUE SPIRALS

Even a cursory inspection of a small sample of images suggests that red spirals may have a significantly higher bar fraction than blue spirals (e.g. Fig. 3). Two of us (BC and KLM) visually inspected the entire face-on discy red spiral sample, along with a similar number of the random mass matched blue spirals. We find that red spirals have an optical bar fraction of at least 67 ± 5 per cent (raw fractions were 72 per cent for BC and 67 per cent for KLM) and up to 100 per cent including more uncertain identifications, while the blue spirals have a bar fraction of only 27 ± 5 per cent (28 per cent from BC and 26 per cent from KLM). These bar identifications used the SDSS *gri* images typically used by Galaxy Zoo, and were based on classic visual bar identification methods such as those used by de Vaucouleurs et al. (1991) to find a bar fraction of 25–30 per cent in the RC3. More recent work on bar fractions in the literature (e.g. Jogee et al. 2004; Barazza, Jogee & Marinova 2008; Sheth et al. 2008; Aguerri, Méndez-Abreu & Corsini 2009) use automated techniques for finding bars using elliptical isophote fitting. The two studies using SDSS data on ∼2000 'disc' galaxies (Barazza et al. 2008; Aguerri et al. 2009) are most directly comparable to this study. Both however use automated techniques to identify disc/spiral samples based largely on concentration (Aguerri et al. 2009) and colour (Barazza et al. 2008, this study does also consider Sersic fits, but the final results are from colour selected 'spirals' only), so we expect systematic differences with our visually identified face-on spiral sample and in particular point out that red spirals by our definition will be completely absent from the Barazza et al. (2008) study, and extremely rare in Aguerri et al. (2009). The overall bar fractions found by Barazza et al. (2008) and Aguerri et al. (2009) are comparable to our total bar fraction of ∼50 per cent (they find 50 and 45 per cent of their disc samples hosting bars), but intriguingly both studies suggest a trend for bluer disc galaxies to be more likely to host bars, in direct contrast to the clear signal we find for red spirals to have more obvious bars in the *gri* images. It is not clear at this point if the difference in these trends is due to the sample selection or the bar identification method [although Aguerri et al. (2009) claim only a 7-per cent difference between their automated bar finder and a visual check of their sample]. A more detailed study of bar fractions in Galaxy Zoo galaxies as a function of various galaxy properties and considering possible biases on the visual bar identification method with *gri* images is being prepared using bar identifications for almost 14 000 spiral galaxies collected during the second phase of Galaxy Zoo (GZ2; Masters et al. 2010b). For the purposes of this work, the huge increase in bar fraction between the blue and red spiral samples gives such a strong hint of a trend of bar fraction with colour (in the sense that red spirals are much more likely to host bars), that it suggests bars may be providing an important clue to the formation of the red spirals and therefore the impact of bars should be considered in a discussion of their possible origin.

In simulations of spiral galaxy formation, bars form quickly once a stable disc is formed, and are difficult to destroy (e.g. Debattista et al. 2006). However, the impact of higher density environments on bars is unclear. Tidal interactions might induce bar formation (e.g. Hernquist & Mihos 1995), but they also act to heat the discs of spirals, and bars form most quickly in cold discs (e.g. Toomre 1964). If external triggers such as tidal interactions are the most important source of bar instabilities, then the higher density environments of the red spirals may naturally lead to high bar fractions.

A possible explanation for the high bar fraction in red spirals could be that the bars themselves are at least partly responsible for

the process which turned off star formation in these objects. Bars are known to be the most efficient way to redistribute material in the discs of galaxies (e.g. Combes & Sanders 1981) by channelling gas into the central regions of the galaxy. Bars have been invoked (e.g. Shlosman et al. 2000) as a way to feed gas to the central black hole – the increase in LINER fraction we observe in the red spirals could be a remnant of this process (if they are LINERs associated with AGN). Perhaps the bars in the red spirals have removed the cold gas from the disc and channelled it inwards where it has either been used as fuel for the AGN or created a starburst. Of course, this starburst must have happened more than $\sim$1 Gyr ago, to be consistent with our observation that red spirals are not post-starburst objects, but if bars are as robust as simulations suggest then they would still persist for a long time after evidence of any bar triggered central starburst was removed.

7 DISCUSSION

Since red spirals are observed at all density levels, the process which creates red spirals cannot be confined only to regions of high galaxy density; environment alone is not sufficient to determine whether a galaxy will become a red spiral or not. The lack of any clear correlation of the star formation rates of red spirals with environment, also indicates that red spirals in low-density regions are similar to those in clusters making it more difficult to invoke only environmental processes in their formation. The process which turns spirals red may be more likely to occur in higher density regions, but must be possible, and proceed in a similar way in all environments, unless completely different mechanisms are responsible for red spirals in high- and low-density regions. That the red spiral population has a significantly higher mean mass than the population of blue spirals, also indicates that they are not uniformly sourced from the field population. However, perhaps the mass transition between red and blue spirals represents the lowest mass spiral which can retain its spiral structure under the influence of environmental effects which shut off its star formation (i.e. low-mass blue spirals might pass through the red spiral phase very quickly or experience both morphological and colour transformation at the same time).

We suggest that, rather than representing an intermediate stage of environmental transformation, red spirals could be 'old spirals' who through normal internal evolution have already used up their reservoirs of gas – perhaps aided by the redistribution of gas due to a bar instability. We suggest that part of the reason they are found to be more common in higher density regions is because the initial density fluctuations decoupled from the Hubble flow earlier there (see Bromm et al. 2009, for a review) and galaxies started assembling at much earlier times (Cooper et al. 2010) in dense environments so have had longer to use up their gas. Such objects would naturally be found at the high mass end of the galaxy distribution as they have been assembling for a long time. Red spirals presumably become less common in the highest densities where strong environmental processes are more important and may have already changed all spirals into early-type galaxies.

It has been shown that for a typical spiral (i.e. with typical star formation rates) to use up all its gas within a Hubble time requires that there is no infall of additional gas from its halo (Larson, Tinsley & Caldwell 1980). Therefore, strangulation (or removal of gas from the outer halo – a process which would be more common in satellite galaxies in higher density regions, but can happen even in low-mass groups Kawata & Mulchaey 2008) is probably required and could by itself create a population of red spirals preferentially found in intermediate density regions (if those in the highest densities were further disrupted). It was observed by Skibba et al. (2009) that the Galaxy Zoo red spirals are preferentially satellite galaxies in massive haloes (while blue spirals are preferentially the central galaxy in a low-mass halo). This observation supports the idea of strangulation as an important part of the mechanism which creates red spirals. In this scenario, they are accreted on to the massive halo as a blue spiral, after which their outer halo gas reservoirs are gently stripped by the main galaxy, and no further accretion of cold gas can take place. Bekki et al. (2002) showed that in such a scenario spiral arms would persist for a few Gyr after the gas was removed. Lower mass spirals presumably are disrupted by gravitational effects in the massive halo and cease to display spiral features, so this model can explain both the mass and environmental distribution of the red spirals.

If other environmental processes are responsible for turning spirals red, they must be very gentle and happen over long time-scales. Continued tidal interactions and/or minor mergers (i.e. galaxy harassment, Moore et al. 1999) could be responsible – these would heat the disc gas above the density required for star formation, but not remove it. If tidal interactions are also responsible for creating bars (e.g. Hernquist & Mihos 1995), the high bar fraction we observe could be a remnant of this (although the bars may still help to shut down star formation by redistributing and heating the gas themselves).

Several authors (e.g. Goto et al. 2003; Wolf et al. 2009) have suggested that red (or passive) spirals are the progenitors of S0 galaxies. The origin of the S0 galaxies has been an on-going debate for more than three decades (Dressler 1980; Moran et al. 2007). S0s are often argued to be too bright and massive and have too large bulge-disc ratios to simply be faded spirals (e.g. Burstein et al. 2005), but Moran et al. (2007) argue that they have linked passive spirals with young S0s in two $z \sim 0.5$ clusters and that a combination of gas stripping and gentle galaxy–galaxy interactions could be responsible for the change, and Driver et al. (2007) show that bulge light is severely attenuated by dust in spiral galaxies which may help to resolve the bulge-disc ratio issue.

There is only one observation in this paper which is immediately in conflict with the idea of the Galaxy Zoo red spirals being the progenitors of S0s. We observe a high optical bar fraction in the face-on discy red spirals, while S0s have a significantly lower bar fraction (Aguerri et al. 2009). Our discy red spirals cannot simply turn into S0s as their spiral arms fade, as the bar instability would remain much longer than the arms. However, in this work, we have purposely selected red spirals with small bulges. Perhaps S0s form from red spirals with large bulges. Further study of the red Galaxy Zoo spirals with large bulges may clear up this issue.

7.1 Future directions

This paper has used optical data from SDSS to reveal the star formation history, dust content, AGN properties, environments and morphologies of a unique sample of intrinsically red disc dominated spiral galaxies. It is clear that significantly more information can be obtained from other surveys, wavelengths and from future theoretical modelling, which will help to shed light on the dominant physical process which formed these objects.

If strangulation is the dominant process forming red spirals they should have almost no residual neutral hydrogen (alternatively, if tidal interactions are responsible by gently heating the disc gas, and thus lowering its density below the threshold for star formation, they should still contain significant quantities of HI). This will be

tested using data from the Arecibo Legacy Fast ALFA (ALFALFA) blind HI survey (Giovanelli et al. 2005) which covers much of the SDSS footprint.

The debate over the nature of the LINER emission could be solved by moving to other wavelengths to reveal the AGN or by obtaining spatially resolved optical spectra to look at the extent of the emission. Deep targeted X-ray observations would reveal objects currently growing their black holes. Unfortunately, currently available public X-ray surveys have too small an area or are at too low luminosity levels to be of use. [For example, the XMM Cluster Survey (XCS; Romer et al. 2001) has only 220 of the blue spirals, and six of the red spirals studied here in its footprint (one blue spiral is detected), while the *ROSAT* All-Sky Survey (Voges et al. 1999) has a high flux limit.] Current radio continuum surveys [for example the National Radio Astronomy Observatory (NRAO)-Very Large Array (VLA) Sky Survey (NVSS); Condon et al. 1998] could also reveal on-going black hole accretion or radio-loud AGN.

More sophisticated modelling of the spectral information (for example from VESPA; Tojeiro et al. 2009) would provide time-resolved star formation histories and more reliable stellar masses. Spatially resolved spectra would additionally allow separate study of the star formation histories of the different regions of these galaxies, and provide dynamical information possibly helpful in determining the role of the bars.

The interpretation of the increased bar fraction in the red spirals is made difficult by the wide range of suggestions of the impact of bars on spiral galaxies. More detailed modelling of spiral galaxies with bars would be extremely helpful in interpreting those observations. We can also use GZ2 data (which ask for a more detailed classification of among other things barred galaxies) to study the more general properties of a large sample of galaxies with bars. For example, studying the environmental dependence of barred galaxies compared to non-barred galaxies would shed light on the role tidal interactions play in bar formation.

8 SUMMARY AND CONCLUSIONS

We study the interesting population of red, or passive, spiral galaxies found by the Galaxy Zoo project. We identify from these red spirals a population of intrinsically red true disc dominated spirals by limiting the sample in inclination (to reduce the impact of dust reddening), requiring that spiral arms be visible, and removing bulge-dominated systems using the SDSS parameter fracDeV. We compare this sample to blue spirals selected in the same way and find as follows.

(i) Red spirals are more likely to be more massive, luminous galaxies than blue spirals. They represent an insignificant fraction of the spiral population at masses below $10^{10}\,M_{\odot}$, but are significant at the highest masses, showing that massive galaxies are red regardless of morphology.

(ii) At the same mass as blue spirals, face-on red spirals do not have larger amounts of dust reddening (as measured by the Balmer decrement), therefore their red colours indicate an ageing stellar population not an increased dust content.

(iii) Red spirals have lower (but not zero) rates of on-going and recent star formation when compared to blue spirals. This is partly related to their higher average mass, however at a fixed mass, red spirals still have less recent star formation than blue spirals.

(iv) As previously observed, red spirals are more common at intermediate local densities (around, or just inside the infall regions of clusters). They are also observed to be more likely than blue spirals to have close neighbours.

(v) Red spirals in all environments have lower rates of recent and on-going star formation than blue spirals, and there are no significant trends of the star formation rates with environment when spirals are split into red/blue. Clearly, the process which creates red spirals is not confined to regions of high galaxy density. So environment alone is not sufficient to determine whether a galaxy will become a red spiral or not.

(vi) Red spirals are more than four times more likely to be classified as Seyfert+LINER/composite objects from their optical spectra than blue spirals. This is partly due to the higher masses of red spirals but is still observed when they are compared to a blue spiral sample selected to have the same mass distribution. We find that a small fraction of low-luminosity AGN are being revealed as the star formation is turned off in the red spirals, but this is not enough to account for all the difference. Most of the difference comes from an increased fraction of LINER-like emission (82 ± 12 per cent of Seyfert/LINERs found in red spirals are LINERs compared to 57 ± 7 per cent in blue spirals).

(vii) Red spirals have significantly higher bar fractions than blue spirals (70 versus 27 per cent), suggesting that bar instabilities and the shutting down of star formation in spirals are correlated.

We propose three possible origins for the red spiral population studied in this work and suggest the most likely explanation is that a combination of the three accounts for the shutting down of their star formation while they retain their spiral structure.

(i) Perhaps red spirals are just old spirals which have used up all of their gas. They are found preferentially in intermediate density regions because structures first start to form at the peaks of the dark matter distribution, but in the centres of clusters spiral morphologies cannot stand up to the environmental disturbances. Red spirals then represent the end stages of spiral evolution irrespective of environment (and in the absence of major mergers) – the spiral version of 'downsizing'.

(ii) Perhaps red spirals are satellite galaxies in massive dark matter haloes. In this scenario, they are accreted on to the halo as a normal blue spiral and have experienced either strangulation (where the gas in their outer haloes has been gently stripped off, and no further cold gas has been allowed to accrete) or harassment (heating their disc gas and preventing further star formation). Low-mass spirals would probably be disrupted in this process and so are not observed as red spirals.

(iii) Perhaps red spirals evolved from normal blue spirals which had bars that were particularly efficient at driving gas inwards. This removed gas from the outer disc and turned the spiral red. If it triggered star formation in the central regions, it must have occurred more than $\sim$1 Gyr ago since red spirals are not post-starburst galaxies.

The red spirals in this work probably cannot be the progenitors of S0s as they have a significantly higher bar fraction than in observed in the S0 population. S0s may however be the end product of red spirals with larger bulges than we have studied here.

ACKNOWLEDGMENTS

This publication has been made possible by the participation of more than 160 000 volunteers in the Galaxy Zoo project. Their contributions are individually acknowledged at http://www.galaxyzoo.org/Volunteers.aspx. KLM acknowledges funding from

the Peter and Patricia Gruber Foundation as the 2008 Peter and Patricia Gruber Foundation International Astronomical Union Fellow, and from the University of Portsmouth and SEPnet (www.sepnet.ac.uk). Support for the work of MM in Leiden was provided by an Initial Training Network ELIXIR (EarLy unIverse eXploration with nIRspec), grant agreement PITN-GA-2008-214227 (from the European Commission). AKR, MM, HCC and RCN acknowledge financial support from STFC. Support for the work of KS was provided by NASA through Einstein Post-doctoral Fellowship grant number PF9-00069 issued by the *Chandra* X-ray Observatory Centre, which is operated by the Smithsonian Astrophysical Observatory for and on behalf of NASA under contract NAS8-03060. CJL acknowledges support from The Leverhulme Trust and the STFC Science In Society Programme. Funding for the SDSS and SDSS-II has been provided by the Alfred P. Sloan Foundation, the Participating Institutions, the National Science Foundation, the US Department of Energy, the National Aeronautics and Space Administration, the Japanese Monbukagakusho, the Max Planck Society and the Higher Education Funding Council for England. The SDSS website is http://www.sdss.org/.

REFERENCES

Adelman-McCarthy J. K. et al., 2008, ApJS, 175, 297
Aguerri J. A. L., Méndez-Abreu J., Corsini, E. M., 2009, A&A, 495, 491
Arnold T. J., Martini P., Mulchaey J. S., Berti A., Jeltema T. E., 2009, ApJ, 707, 1691
Baldry I. K., Balogh M. L., Bower R. G., Glazebrook K., Nichol R. C., Bamford S. P., Budavari T., 2006, MNRAS, 373, 469
Baldwin J. A., Phillips M. M., Terlevich R., 1981, PASP, 93, 5 (BPT)
Ball N. M., Loveday J., Brunner R. J., 2008, MNRAS, 383, 907
Balogh M. L., Morris S. L., Yee H. K. C., Carlberg R. G., Ellingson E., 1999, ApJ, 527, 54
Bamford S. P., Rojas A. L., Nichol R. C., Miller C. J., Wasserman L., Genovese C. R., Freeman P. E., 2008, MNRAS, 391, 607
Bamford S. P. et al., 2009, MNRAS, 393, 1324
Barazza F. D., Jogee S., Marinova I., 2008, ApJ, 675, 1194
Bekki K., Couch W. J., Shioya Y., 2002, ApJ, 577, 651
Binette L., Magris C. G., Stasińska G., Bruzual A. G., 1994, A&A, 292, 13
Bruzual G., Charlot S., 2003, MNRAS, 344, 1000
Boselli A., Gavazzi G., 2006, PASP, 118, 517
Bower R. G., Benson A. J., Malbon R., Helly J. C., Frenk C. S., Baugh C. M., Cole S., Lacey C. G., 2006, MNRAS, 370, 645
Bromm V., Yoshida N., Hernquist L., McKee C. F., 2009, Nat, 459, 49
Bundy K. et al., 2006, ApJ, 651, 120
Bundy K. et al., 2010, ApJ, submitted (arXiv:0912.1077)
Burstein D., Ho L. C., Huchra J. P., Macri L. M., 2005, ApJ, 621, 246
Cid Fernandes R., Heckman T., Schmitt H., González Delgado R. M., Storchi-Bergmann T., 2001, ApJ, 558, 81
Combes F., Sanders R. H., 1981, A&A, 96, 164
Condon J. J., Cotton W. D., Greisen E. W., Yin Q. F., Perley R. A., Taylor G. B., Broderick J. J., 1998, AJ, 115, 1693
Conselice C. J., 2006, MNRAS, 373, 1389
Cooper M. C., Gallazzi A., Newman J. A., Yan R., 2010, MNRAS, 402, 1942
Cooray A., 2005, MNRAS, 363, 337
Cortese L., Hughes T. M., 2009, MNRAS, 400, 1225
Couch W. J., Barger A. J., Smail I., Ellis R. S., Sharples R. M., 1998, ApJ, 497, 188
Cowie L. L., Songaila A., 1977, Nat, 266, 501
Croton D. J. et al., 2006, MNRAS, 365, 11
Croton D. J., Norberg P., Gaztañaga E., Baugh C. M., 2007, MNRAS, 379, 1562
Debattista V. P., Mayer L., Carollo C. M., Moore B., Wadsley J., Quinn T., 2006, ApJ, 645, 209
Deng X.-F., He J.-Z., Wu P., Ding Y.-P., 2009, ApJ, 699, 948
de Vaucouleurs G., de Vaucouleurs A., Corwin H. G. Jr, Buta R. J., Paturel G., Fouqué P., 1991, Third Reference Catalogue of Bright Galaxies. Springer, New York
Dressler A., 1980, ApJ, 236, 351
Dressler A., Smail I., Poggianti B. M., Butcher H., Couch W. J., Ellis R. S., Oemler A. Jr, 1999, ApJS, 122, 51
Driver S. P., Popescu C. C., Tuffs R. J., Liske J., Graham A. W., Allen P. D., de Propris R., 2007, MNRAS, 379, 1022
Gallazzi A. et al., 2009, ApJ, 690, 1883
Giovanelli R. et al., 2005, AJ, 130, 2598
Glazebrook K. et al., 2004, Nat, 430, 181
Gnedin O. Y., 2003, ApJ, 582, 141
Goto T., Yamauchi C., Fujita Y., Okamura S., Sekiguchi M., Smail I., Bernardi M., Gomez P. L., 2003, MNRAS, 346, 601
Granato G. L., De Zotti G., Silva L., Bressan A., Danese L., 2004, ApJ, 600, 580
Gunn J. E., Gott J. R. I., 1972, ApJ, 176, 1
Heckman T. M., 1980, A&A, 87, 152
Hernquist L., Mihos J. C., 1995, ApJ, 448, 41
Ho L. C., 2008, ARA&A, 46, 475
Hopkins P. F. et al., 2009, MNRAS, 397, 802
Hughes T. M., Cortese L., 2009, MNRAS, 396, L41
Ishigaki M., Goto T., Matsuhara H., 2007, MNRAS, 382, 270
Jogee S. et al., 2004, ApJ, 615, L105
Kauffmann G. et al., 2003a, MNRAS, 341, 33
Kauffmann G. et al., 2003b, MNRAS, 346, 1055
Kawata D., Mulchaey J. S., 2008, ApJ, 672, L103
Kewley L. J., Dopita M. A., Sutherland R. S., Heisler C. A., Trevena J., 2001, ApJ, 556, 121
Kewley L. J., Groves B., Kauffmann G., Heckman T., 2006, MNRAS, 372, 961
Lamastra A., Bianchi S., Matt G., Perola G. C., Barcons X., Carrera F. J., 2009, A&A, 504,73
Larson R. B., Tinsley B. M., Caldwell C. N., 1980, ApJ, 237, 692
Lin C. C., Shu F. H., 1964, ApJ, 140, 646
Lintott C. J. et al., 2008, MNRAS, 389, 1179
Liske J., Lemon D. J., Driver S. P., Cross N. J. G., Couch W. J., 2003, MNRAS, 344, 307
Lee J., Pen U.-L., 2007, ApJ, 670, L1
Lee J. H., Lee M. G., Park C., Choi Y.-Y., 2008, MNRAS, 389, 1791
Lee J. H., Lee M. G., Park C., Choi Y.-Y., 2010, MNRAS, in press (arXiv:0911.4386)
Mahajan S., Raychaudhury S., 2009, MNRAS, 400, 687
Maraston C., 2005, MNRAS, 362, 799
Masters K. L. et al., 2010a, MNRAS, in press (arXiv:1001.1744)
Masters K. L. et al., 2010b, MNRAS, submitted (astro-ph/1003.0449)
Mignoli M. et al., 2009, A&A, 493, 39
Miller C. J., Nichol R. C., Gómez P. L., Hopkins A. M., Bernardi M., 2003, ApJ, 597, 142
Moore B., Lake G., Quinn T., Stadel J., 1999, MNRAS, 304, 465
Moran S. M., Ellis R. S., Treu T., Salim S., Rich R. M., Smith G. P., Kneib J.-P., 2006, ApJ, 641, L97
Moran S. M., Ellis R. S., Treu T., Smith G. P., Rich R. M., Smail I., 2007, ApJ, 671, 1503
Okamoto T., Nemmen R. S., Bower R. G., 2008, MNRAS, 385, 161
Osterbrock D. E., 1989, Astrophysics of Gaseous Nebulae and Active Galactic Nuclei. University Science Books, Mill Valley, CA
Poggianti B. M., Smail I., Dressler A., Couch W. J., Barger A. J., Butcher H., Ellis R. S., Oemler A. Jr, 1999, ApJ, 518, 576
Romer A. K., Viana P. T. P., Liddle A. R., Mann R. G., 2001, ApJ, 547, 594
Salimbeni S. et al., 2008, A&A, 477, 763
Sarzi M. et al., 2010, MNRAS, 402, 2187
Schawinski K. et al., 2006, Nat, 442, 888
Schawinski K., Thomas D., Sarzi M., Maraston C., Kaviraj S., Joo S.-J., Yi S. K., Silk J., 2007, MNRAS, 382, 1415
Schawinski K. et al., 2009a, ApJ, 690, 1672
Schawinski K. et al., 2009b, MNRAS, 396, 818

Table A1. A sample of face-on, 'discy' red spirals. (The full table is available in the online version of the paper – see Supporting Information.)

SDSS objid	RA (J2000, °)	Dec. (J2000, °)	Redshift	M_r	$(g-r)$	'Redness'	$\log(a/b)$	fracDeV
587731186741346415	1.218164	0.351724	0.0833	-21.26 ± 0.01	0.695 ± 0.020	0.040	0.144	0.42
588015509270364319	2.277073	0.042422	0.0735	-21.75 ± 0.01	0.701 ± 0.021	0.036	0.143	0.46
587731187279265981	3.718539	0.634254	0.0642	-21.15 ± 0.01	0.756 ± 0.039	0.103	0.042	0.00
587731187279331410	3.771462	0.642945	0.0621	-21.50 ± 0.01	0.662 ± 0.017	0.002	0.179	0.32
588015508734148754	3.789492	−0.366536	0.0661	-22.18 ± 0.01	0.687 ± 0.018	0.013	0.070	0.40
...	...	...	...	..	...	...	...	...

Table A2. A sample of face-on, 'discy' blue spirals. (The full table is available in the online version of the paper – see Supporting Information.)

SDSS objid	RA (J2000 °)	Dec. (J2000 °)	Redshift	M_r	$(g-r)$	'Redness'	$\log(a/b)$	fracDeV
587727225690259639	0.276560	−10.400263	0.0754	-21.41 ± 0.01	0.434 ± 0.020	−0.225	0.084	0.12
587727225690259660	0.325174	−10.426144	0.0767	-21.03 ± 0.02	0.561 ± 0.028	−0.090	0.078	0.07
587730773888991473	0.566363	14.671807	0.0834	-20.91 ± 0.02	0.503 ± 0.035	−0.145	0.106	0.06
588015510343385206	0.665200	0.942673	0.0807	-22.38 ± 0.01	0.632 ± 0.018	−0.046	0.079	0.22
588015510343516321	0.941711	0.854914	0.0611	-20.69 ± 0.01	0.378 ± 0.023	−0.266	0.185	0.00
...	...	...	...	..	...	...	...	...

Schawinski K. et al., 2010, ApJ, 711, 284
Sheth K. et al., 2008, ApJ, 675, 1141
Shlosman I., Peletier R. F., Knapen J. H., 2000, ApJ, 535, L83
Silk J., 2005, MNRAS, 364, 1337
Simien F., de Vaucouleurs G., 1986, ApJ, 302, 564
Simon P., Hetterscheidt M., Wolf C., Meisenheimer K., Hildebrandt H., Schneider P., Schirmer M., Erben T., 2009, MNRAS, 1058
Skibba R. A. et al., 2009, MNRAS, 399, 966
Smolčić V., 2009, ApJ, 699, L43
Sorrentino G., Radovich M., Rifatto A., 2006, A&A, 451, 809
Stasińska G., Vale Asari N., Cid Fernandes R., Gomes J. M., Schlickmann M., Mateus, A., Schoenell W., Sodré L. Jr, 2008, MNRAS, 391, L29
Strauss M. A. et al., 2002, AJ, 124, 1810
Tojeiro R., Wilkins S., Heavens A. F., Panter B., Jimenez R., 2009, ApJS, 185, 1
Toomre A., 1964, ApJ, 139, 1217
Toomre A., Toomre, J., 1972, ApJ, 178, 623
Tremonti C. A. et al., 2004, ApJ, 613, 898
van den Bergh S., 1976, ApJ, 206, 883
Veilleux S., Osterbrock D. E., 1987, ApJS, 63, 295
Voges W. et al., 1999, A&A, 349, 389
Walker I. R., Mihos J. C., Hernquist L., 1996, ApJ, 460, 121
Wolf C., Gray M. E., Meisenheimer K., 2005, A&A, 443, 435
Wolf C. et al., 2009, MNRAS, 393, 1302

APPENDIX A: SAMPLE OF DATA TABLES

We provide, in this Appendix, samples of the data tables we make available electronically listing important information (all based on SDSS data) for both our red (Table A1) and blue (Table A2) face-on discy spiral samples. In both tables, columns are (1) SDSS objid; (2) and (3) RA and Dec. in J2000 decimal degrees; (4) Redshift; (5) Absolute r-band (Petrosian) magnitude, M_r; (6) $(g-r)$ colour (from model magnitudes); (7) 'redness', defined as the distance in magnitudes from the blue limit of the $(g-r)$ verses M_r red sequence (see equation 1 in Section 2.1); (8) axial ratio, $\log(a/b)$ from the r-band isophotal measurement and (9) fracDeV; the fraction of the best-fitting light profile made up by a de Vaucouleur profile (as opposed to an exponential disc).

SUPPORTING INFORMATION

Additional Supporting Information may be found in the online version of this article:

Table A1. A sample of face-on, 'discy' red spirals.
Table A2. A sample of face-on, 'discy' blue spirals.

Please note: Wiley-Blackwell are not responsible for the content or functionality of any supporting materials supplied by the authors. Any queries (other than missing material) should be directed to the corresponding author for the article.

This paper has been typeset from a TEX/LATEX file prepared by the author.